

# POLITECNICO DI TORINO

MASTER OF SCIENCE IN  
MECHATRONIC ENGINEERING



Master Degree Thesis

## LQI control of dual-clutch transmission systems in hybrid vehicles with P2 architecture

Supervisors:

Prof. CARLO NOVARA

Ing. EMANUEL CORIGLIANO

Candidate:

ILARIA GIRONE

JULY 2020



# Summary

In this dissertation, realized in collaboration with Centro Ricerche Fiat (CRF), a Linear Quadratic Integral approach is implemented in order to control a Dry Dual Clutch Transmission system in hybrid vehicles with P2 architecture, during the slipping phase. The main objectives of the control are related to an improvement of the vehicle comfort, drivability and robustness; a better gearbox/clutch maneuver smoothness and the minimization at the same time of vibrations and abrupt movements. In particular, the analysis is focused on the Dry Dual Clutch Transmission (DDCT) developed by Fiat Power-train Technologies. The aim of the control is that to ensure the slipping speed, that is the speed difference between the disks of the clutch, reaches the zero value in a smooth way, after following a given reference. A simplified model of the transmission is here implemented with clutch actuator, dynamic engine model and elasticity of the transmission shafts. Some uncertainties have to be considered in the control: the delays of the clutch and engine actuators, the clutch transmissibility, vehicle mass and the drive shaft torsion effects.

Firstly a Linear Quadratic Integral controller for the plant without actuators is simulated: both the engine and clutch torques are considered as inputs computed by the controller and the outputs are equal to the states: engine speed, slipping speed, drive shaft torsional speed and angle.

Then, with the aim of improving the model making it more realistic, the actuators and delays are introduced in the model and some techniques are introduced together with the LQI control strategy in order to compensate them, obtaining a more complex state space representation of the plant that in this case, being more accurate, gives more reliable results.

The impossibility to measure the actuators states, makes necessary the introduction of a state estimation with the Kalman Filter that results to be the best way to manage the uncertainties related to the presence of the delays.

In conclusion, the Linear Quadratic Integral approach for the clutch slipping control turns out to be advantageous in terms of performances that are assessed in terms of Standard deviation and Root Mean Square Error (RMSE) and also for its flexibility that makes possible the introduction of other control strategies suitable for the actuators management.



# Acknowledgements

*Preme ergo quod coepisti,  
et fortasse perduceris aut ad summum  
aut eo quod summum nondum esse solus intellegas  
Seneca, Epistulae morales ad Lucilium, Liber II*

La stesura della tesi di laurea rappresenta la conclusione del percorso universitario: tante sono state in questi anni le esperienze e le difficoltà vissute, che hanno certamente consentito una crescita non solo dal punto di vista professionale ed accademico, ma anche una grandissima maturazione personale.

Ringrazio il Prof. Carlo Novara, relatore della presente tesi e il correlatore Ing. Emanuel Corigliano per avermi dato l'opportunità di occuparmi di un progetto dai caratteri innovativi, grazie per la straordinaria disponibilità e supporto che mi hanno accompagnata negli ultimi mesi. Un ringraziamento speciale ai miei genitori che nonostante ogni difficoltà mi hanno sempre spronata ad andare avanti con forza e determinazione, che mi hanno insegnato il valore del sacrificio e hanno sempre gioito con me al raggiungimento di ogni singolo obiettivo, grazie per avermi sempre accompagnata, seppur talvolta da lontano, in ciascun istante della mia esperienza universitaria e non solo.

Un grazie a mia madre, per me esempio di coraggio e grinta, che mi ha insegnato che la forza d'animo consente di superare ogni avversità anche la più ardua.

Un grazie al mio papà, che ha da sempre fatto in modo che seguissi i miei desideri ed inclinazioni ed ha sempre guardato con orgoglio ed ammirazione ciascun mio traguardo.

Un ringraziamento a chi mi ha accompagnata in questi cinque anni, chi c'è sempre stato e chi è andato via, ma anche le persone che ho incontrato in questo percorso e con le quali ho potuto avere sempre un confronto costruttivo di condivisione.

Ringrazio gli amici di sempre, per avermi sempre ascoltata, grazie perché mi siete stati sempre vicini e avete cercato di incoraggiarmi nei momenti più difficili, vi sarò per sempre grata.



# Table of Contents

<b>List of Tables</b>	VIII
<b>List of Figures</b>	IX
<b>1 Introduction</b>	1
1.1 Thesis structure . . . . .	3
<b>2 DCT System in hybrid vehicles with P2 architecture</b>	4
2.1 Introduction . . . . .	4
2.2 C635 Dry Dual Clutch Transmission . . . . .	9
2.2.1 Operation of the DDCT . . . . .	11
2.2.2 Dry Dual Clutch Unit . . . . .	12
2.2.3 Electro-hydraulic actuation system . . . . .	13
2.2.4 DDCT Control Unit . . . . .	14
2.3 Micro slip . . . . .	16
2.4 State of art . . . . .	17
2.5 Model configuration . . . . .	19
2.5.1 Actuators . . . . .	20
2.5.2 Engine model . . . . .	21
2.5.3 Load . . . . .	21
2.6 Hybrid electric vehicles with P2 architecture . . . . .	23
<b>3 Model Analytical description</b>	25
3.1 Introduction . . . . .	25
3.2 State Space representation . . . . .	26
3.3 Complete model with actuators . . . . .	29
<b>4 LQI technique</b>	32
4.1 Linear Quadratic regulator . . . . .	32
4.1.1 Finite-horizon, continuous-time LQR . . . . .	32
4.1.2 Infinite-horizon, continuous-time LQR . . . . .	33

4.1.3	Finite-horizon, discrete-time LQR . . . . .	33
4.1.4	Infinite-horizon, discrete-time LQR . . . . .	34
4.2	Incorporating integral action in LQR . . . . .	34
4.3	Optimal management of the delays . . . . .	37
4.3.1	Smith Predictor . . . . .	38
4.3.2	Kalman state observer . . . . .	40
4.4	LQI in Simulink . . . . .	42
4.5	Plant without actuators and delays . . . . .	43
<b>5</b>	<b>Tuning and Simulation results</b>	<b>49</b>
5.1	LQI technique with actuators and delays . . . . .	49
5.2	Linearization of the actuators and delays . . . . .	54
5.3	LQI technique with Smith Predictor . . . . .	58
5.4	State space representation of the actuators and the Plant with LQI technique . . . . .	61
5.5	Kalman State Estimation . . . . .	64
5.6	Comparison between simulation results . . . . .	68
5.6.1	Observations . . . . .	69
<b>6</b>	<b>Conclusions</b>	<b>70</b>
6.1	Future works . . . . .	71
	<b>Bibliography</b>	<b>72</b>

# List of Tables

2.1	C635 DDCT Main Mechanical characteristics . . . . .	9
3.1	DDCT main parameters . . . . .	27
5.1	Indexes computation . . . . .	68
5.2	Convergence interval . . . . .	68

# List of Figures

2.1	The basic configurations of HEVs . . . . .	4
2.2	MHEV system . . . . .	5
2.3	MHEV with P2 architecture . . . . .	7
2.4	C635 Manual Transmission and DDCT . . . . .	8
2.5	Cross section of the C635 DDCT . . . . .	10
2.6	Dual Clutch Unit, Clutch Actuators and installation . . . . .	12
2.7	Hydraulic Power Unit and CAM . . . . .	13
2.8	C635 DDCT complete actuation system . . . . .	14
2.9	DCT and clutches K1 and K2 . . . . .	16
2.10	Schematic representation of the DDCT . . . . .	16
2.11	Decoupling control implemented in [4] . . . . .	17
2.12	MPC control from [5] . . . . .	18
2.13	Engine speed and torque control [6] . . . . .	18
2.14	General scheme presented in [7] . . . . .	19
2.15	Overall model of the DDCT system . . . . .	20
2.16	Actuators for $C_m$ and $C_f$ . . . . .	20
2.17	Reference angular velocity . . . . .	21
3.1	General driveline scheme . . . . .	25
3.2	DDCT driveline scheme . . . . .	26
3.3	Reduced linear driveline scheme . . . . .	26
3.4	Complete model with actuators . . . . .	30
4.1	General LQI scheme . . . . .	35
4.2	General architecture for the control . . . . .	37
4.3	Controller without Smith Predictor . . . . .	39
4.4	System considered for Smith Predictor . . . . .	39
4.5	Smith Predictor . . . . .	40
4.6	General observer scheme . . . . .	41
4.7	LQI controller scheme . . . . .	42
4.8	Plant without actuators . . . . .	44

4.9	General scheme with controller . . . . .	44
4.10	Delta speed behavior without actuators . . . . .	45
4.11	Drive shaft torsion speed and angle . . . . .	45
4.12	Delta speed behavior without actuators T=10ms . . . . .	46
4.13	Drive shaft torsion speed and angle T=10 ms . . . . .	46
4.14	Total engine and clutch torque T=10 ms . . . . .	47
5.1	Plant fed with the actuated inputs . . . . .	49
5.2	Delta speed behavior . . . . .	50
5.3	Drive shaft torsion speed and angle . . . . .	50
5.4	Total engine and clutch torque . . . . .	51
5.5	Delta speed behavior with T=10 ms . . . . .	52
5.6	Drive shaft torsion speed and angle with T=10 ms . . . . .	52
5.7	Total engine and clutch torque with T=10 ms . . . . .	53
5.8	Model plant to be linearized . . . . .	54
5.9	Delta speed behavior with linearization . . . . .	55
5.10	Drive shaft torsion speed and angle with linearization . . . . .	55
5.11	Total engine and clutch torque with linearization . . . . .	56
5.12	Delta speed behavior with linearization T=10 ms . . . . .	57
5.13	Drive shaft torsion speed and angle with linearization T=10 ms . . . . .	57
5.14	Total engine and clutch torque with linearization T=10 ms . . . . .	58
5.15	Smith Predictor scheme for clutch actuator . . . . .	58
5.16	Delta speed behavior with LQI and Smith Predictor . . . . .	59
5.17	Drive shaft torsion speed and angle with LQI and Smith Predictor . . . . .	59
5.18	Total engine and clutch torque with LQI and Smith Predictor . . . . .	60
5.19	Simulink scheme of the complete system . . . . .	61
5.20	Delta speed behavior with LQI and complete State Space . . . . .	62
5.21	Drive shaft torsion speed and angle with complete State Space . . . . .	62
5.22	Total engine and clutch torque with LQI and complete State Space . . . . .	63
5.23	LQI with Kalman filter . . . . .	64
5.24	Full model with observer . . . . .	65
5.25	Plant with actuators . . . . .	65
5.26	Delta speed behavior with LQI and Kalman filter . . . . .	66
5.27	Drive shaft torsion speed and angle and Kalman filter . . . . .	66
5.28	Total engine and clutch torque with LQI with Kalman filter . . . . .	67
5.29	Expected performance . . . . .	67



# Chapter 1

## Introduction

The automotive industry is facing many challenges related to different fields, in particular it is becoming more and more important the improvement of the technologies related to the reduction of emissions, fuel consumption and driving comfort. Considering all these factors, that are becoming crucial for the success of a new product, the companies are giving particular attention to the development of more efficient transmission systems.

The environmental needs and legislative pressure for a significant CO<sub>2</sub> emissions reduction in the coming years forces the automotive industry to optimize every single component of the next generation vehicles. [1]

The transmission, which is the element used for matching the engine's characteristics with the vehicle drivability requirements, assumes an important role in this optimization process. High mechanical efficiency and the ability to enable the operation of the prime mover in its most efficient operating points while delivering the required power are clearly the main development objectives of any new transmission projects.

The Manual Transmission, despite its intrinsically high overall efficiency which can also benefit of the related dry clutches technology, cannot guarantee high Real-life powertrain efficiency due to the impossibility to control it in coordination with the rest of the powertrain and vehicle.

The step necessary to ensure this possibility involves transmission automation, leading to the adoption of a Non Manual Transmission (NMT) technology. Premising that the specific market, brand, mission and user requirements must be taken into account for the proper transmission choice, the conclusion is that there is no single Non Manual Transmission technology able to satisfy all vehicle, market, mission and user requirements:

- AMTs (Automated Manual Transmissions) are the most cost-effective solutions for transmission automation and are suitable for utilitarian vehicle applications
- DCTs (Dual Clutch Transmissions) represent a perfect balance between powertrain efficiency and driving comfort and are suitable for medium segment applications, furthermore thanks to sportiveness' driving experience that they can transmit to the driver are now one of the preferred choice for sports cars.
- CVTs (Continuously Variable Transmissions) are particularly suitable for some specific market and vehicle segments.
- Multi-speed ATs (planetary Automatic Transmissions) are competitive in terms of comfort/performance for the higher segment vehicles.

In this thesis project, the DCT transmission system is taken into account, especially because it allows the engine's energy to flow directly to the wheels. On the other hand, the driver comfort also depends on the way in which the clutches engage: this engagement must be realised as smooth as possible.

Adopting some specific control strategies, it is possible to reduce vibrations and abrupt movements, managing the transitions between combustion engine and electric engine and improving the clutch maneuver smoothness.

The clutch engagement problem is here analysed, focusing on the Dual Clutch Transmission (DCT) system, in the following operational conditions: one DCT clutch is in slipping phase, the other is opened, while the combustion engine is ON.

The LQI (Linear Quadratic Integral) control is used in order to control the dual clutch during the slipping phase making possible the convergence to zero of the speed difference between the clutch disks (delta speed).

## **1.1 Thesis structure**

The second chapter of this dissertation deals with the explanation of the characteristics of the Dual Clutch transmission system in hybrid vehicles with P2 architecture, the description of the main components involved and the control targets.

Then, in the following chapter the micro-slip problem is presented, the state of art and the detailed model configuration, together with the analytical description of the system, the equations developed and the determined state space representation.

The fourth chapter is reserved to the description of the LQI control strategy, the operational conditions and the control targets. Here, also the other techniques adopted in order to compensate the delays of the actuators are explained, paying specific attention to the advantages of combining different methods to obtain better results in terms of outputs.

In the last part of the thesis, the system realized in Simulink environment is shown, along with the simulation results that are interpreted and commented. A detailed description is carried out for the different strategies adopted.

In the last chapter the conclusions about the obtained results are exhibited with all the consideration needed to validate the improvement of the transmission system, achieving the control targets.

## Chapter 2

# DCT System in hybrid vehicles with P2 architecture

### 2.1 Introduction

Nowadays, one of the aims of the automotive industry is a more efficient use of energy in a vehicle. Hybrid vehicles are possible candidates to reduce both emissions and consumptions. Hybrid powertrains utilize a conventional ICE together with a battery, an electric motor, and an electronic controller. HEVs have two possible configurations: series and parallel hybrids.

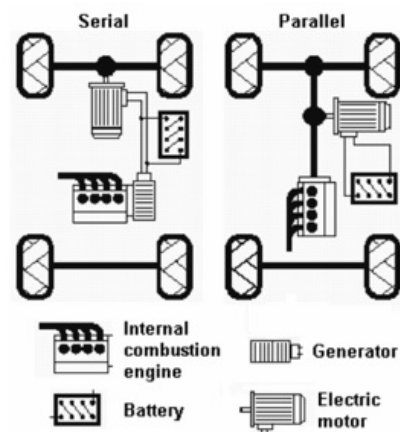


Figure 2.1: The basic configurations of HEVs

In the series structure, the ICE is exploited to drive an alternator to generate electricity, which is then sent directly to the electric motor, which powers the wheels or can be stored in a battery system. The engine is not giving power directly to the wheels and its efficiency is maximised because it operates within a small range of speeds. The parallel hybrid has two paths for the power, so that the wheels can be directly powered by either the Integrated Electric Machine or the electric motor (or both).

The fuel consumption is reduced and power output does not change because the electric motor and the battery provide added power to the ICE. In order to save fuel, the engine automatically stops when the vehicle comes to a stop, and starts automatically when accelerating again. The battery is recharged using the energy from the regenerative braking, avoiding the IEC from doing it, and saving more fuel. A hybrid powertrain does not need to be plugged in and charged up because it is completely self-sufficient.

There is another, simpler version of the hybrid powertrain that is the so-called "mild hybrid", which has an electronically controlled integrated starter-generator (ISG), instead of an electric propulsion motor and is also capable of efficient heavy-duty towing. [2] The ISG is not able to move the car, but it can help its propulsion and recover energy through regenerative braking. The mild hybrid cars are normally operated in the same manner as the full hybrids. One of the differences with respect to a full hybrid is that a mild hybrid has a much smaller battery than a full hybrid and cannot run on battery power alone.

A typical mild hybrid vehicle system's structure is given below:

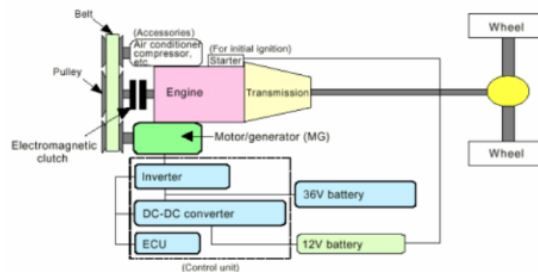


Figure 2.2: MHEV system

One of the most important advantages of the mild HEV system is that its cost is lower compared to the full HEV system. For sure, a less expensive hybrid system is more likely to appeal to a greater number of simple consumers who do not need more robust and more expensive hybrid systems, especially in the initial phase of market development. When consumers will better understand the differences in hybrid technologies, they will be better able to match their need for increased fuel saving with the most cost-effective system.

Presently, the most common mild hybrid topology is the P0 architecture, in which the electric machine is integrated in the Front End Accessory Drive (FEAD). In this case, the electric machine is replacing the alternator in terms of usage.

The belt-integrated starter generator (BiSG or e-machine) can be an asynchronous or synchronous electric machine, and it has two main functions:

1. provide torque to the powertrain in motor mode
2. produce electricity in generator mode

For example, a BiSG can provide 4-6 kW of nominal power and around 14-16 kW of peak power. The output torque can be around 60 Nm which can reach up to 160 Nm at the crankshaft when amplified by the belt pulley ratio.

In case of a P1 mild hybrid architecture, the e-machines need to be flat, in order to be positioned between the internal combustion engine and the transmission. For these applications, in order to have a high torque output, the e-machines need to have high power density. Therefore permanent magnet synchronous e-machines are used instead of induction asynchronous e-machines.

Moving the electric motor between the engine and the transmission the architecture becomes P2. The change from P1 to P2, realized also introducing a clutch that disconnects the thermal engine, realizes many possibilities for hybrid cars.

It is possible, for example, to improve existing transmissions, for example using the electric motor group – clutch instead of the torque converter.

Effectively, the electric motor is connected to the input of the transmission and gives energy instead of the thermal one. The clutch gives the possibility to start the combustion engine, start from a standstill and travel in electric mode without pulling it. The P2 system also allows the hybrid car to "boot" with only the electric motor and thermal engine turned off.

The P3 configuration changes the position of the engine "downstream" of the gearbox. It minimizes losses, as the electric motor drags only the final part of the transmission. However, this kind of solution is a bit expensive because it forces to change the design of a large part of the transmission.

Hybrid cars with the acronym P4 have an electric motor that acts exclusively on the axis not connected to the thermal engine. In this way it is possible to have a four-wheel drive without mechanical connection with the thermal engine. Even the pure electric mode is easily achieved, just disconnecting the "main" transmission using only the axle connected to the electric motor.

Considering the P2 architecture, it is possible to employ the Dual Clutch Transmission (DCT), in order to solve the problem of the torque interruption during the automated gear shifting of the Automated Manual Transmissions (AMT) that penalizes the comfort of the driver.

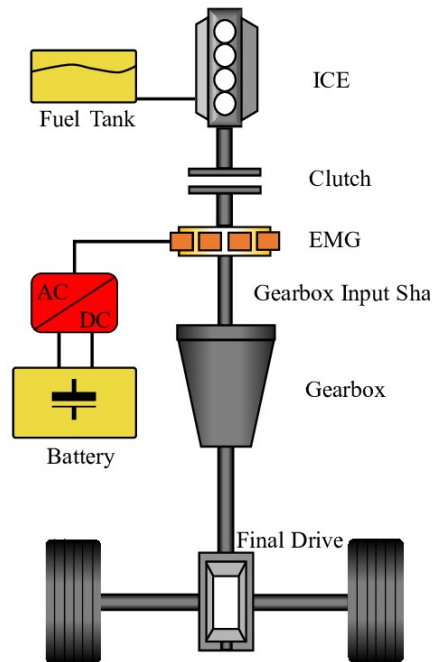


**Figure 2.3:** MHEV with P2 architecture

The Dual Clutch Transmission is made-up of two independent sub-gearboxes, one for the even gear sets and the other for the odd gear sets, each one activated by separate clutches: the engaging and the disengaging ones. The gear shift process involves the engagement of the on-coming clutch and the release of the off-going clutch to ensure a shift without traction interruption.

There are two different kinds of DCTs: two wet multi-disc clutches bathed in oil for cooling (WDCT), or two dry single-disc clutches (DDCT). Wet Dual Clutch Transmissions are usually used in high torque applications, while the Dry-Dual Clutch is employed for smaller vehicles where lower torques are needed.

In this thesis project the Dry Dual Clutch Transmission is considered, in particular the transmission developed by Fiat Power-train Technologies that is part of the new C365 transmission family. This new transmission family consists of a range of Manual, All Wheel Drive and DCT transversal, 6-speed transmissions with a maximum input torque of 350 Nm and output torque of 4200 Nm. The DCT version of this transmission is the highest rated amongst the double dry dual clutch transmissions in the market. The C365 transmissions have been designed taking into account the current trends in vehicle and powertrain technology.

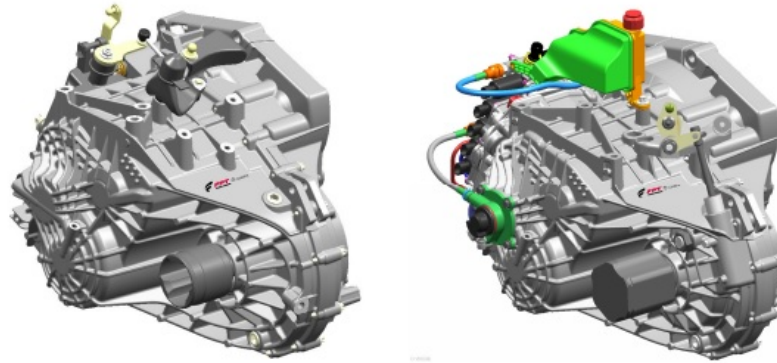


**Figure 2.4:** C635 Manual Transmission and DDCT

The advantage of employing the dry clutch instead of the wet dual clutch is related to the improvement of the fuel efficiency, that is directly linked to the reduction of pumping losses of the fluid in the clutch housing. This research takes into account the development of a control method in order to track a reference trajectory for the clutch slipping speed avoiding oscillations, through LQI Linear Quadratic Integral control strategy. The adoption of other techniques together with the main one has been necessary in order to manage the delays of the clutch and motor actuators.

## 2.2 C635 Dry Dual Clutch Transmission

The C635 Dry Dual Clutch Transmission is a six-speed, automated manual gearbox developed by Fiat Powertrain Technologies (FPT) together with Magneti Marelli and BorgWarner, and is fabricated by FPT at the Verrone, Italy plant. The transmission adopts a control system developed by Magneti Marelli that incorporates BorgWarner’s hydraulic actuation module into its own power and transmission control units. The DDCT is sold in different ways under the trade names TCT, Twin Clutch Transmission (Alfa Romeo), Euro Twin Clutch Transmission (Fiat USA), and Dual Dry Clutch Auto Transmission (Dodge).

This transmission is the highest-torque transverse dry dual clutch application and it is able to receive torque inputs of up to 350 Nm and realizes a maximum output of 4200 Nm. It weights 81 kg, inclusive of oil and transmission control unit. The C635 DDCT transmission mechanical characteristics are summarised in Table 1:

Layout	3-shaft plus RG idler	
Number of speeds	6-7	
Housing	Two piece with intermediate support plate	
P-D Centre Distance	197mm	
Input Torque	350 Nm max.	
Output Torque	4200 Nm max.	
Gears	Ratios in production	Torque Limitations
I	3.9	260 Nm
II	2.269	295 Nm
III	1.435-1.522	350 Nm
IV	0.978-1.116	350 Nm
V	0.755-0.915	350 Nm
VI	0.622-0.767	350 Nm
RG	4.00	250 Nm
Final Drive	3.579-3.833-4.118-4.438	
Maximum speed ratio in I	17.3	
Spread	6.27	
Synchronisers	I-II-III	3-cone
	IV-RG	2-cone
	V-VI	1-cone
Weight	81 kg	with hydraulic and lubrication oil

**Table 2.1:** C635 DDCT Main Mechanical characteristics

As shown in Figure 2.5 below, the 3-shaft transmission architecture is contained in a 2-piece aluminium housing with an intermediate support plate for the shaft bearings. This solution allows the positioning of the differential group closer to the engine.

The gear set housing is characterised by reduced upper secondary shaft length, a feature which is also necessary in order to ensure packaging in the lower segment vehicles where the longitudinal crash beam imposes serious installation constraints. The 6th gear is shared with the 4th while an eventual, non-powershift, 7th gear

would be shared with the 5th, with either increased or equal overall gear spread compared to the 6-speed version. The most important feature of this transmission in terms of packaging characteristics is the adoption of a coaxial pull-rod for the actuation of the odd-gear clutch (K1), while the even gear clutch (K2) is actuated with a rather conventional hydraulic Concentric Slave Cylinder (CSC). This pull-rod is connected to a hydraulic piston actuator located on the rear face of the transmission housing in a manner identical to the one adopted in the past in an earlier Fiat Powertrain technical demonstrator. In fact, despite the optimised axial dimension of the dry Dual Clutch Unit (DCU) the eventual addition of a second actuator mechanism within the clutch housing would prohibit installation of the transmission in the lower Segment vehicles. Finally, all synchroniser groups share the same base elements and are identical to those of the Manual version. Logistics and economical considerations favoured this solution which may not be necessary in a DCT transmission. The four forks are guided on two rods. A specific form of the rods allows production of a single part number, sheet metal, fork body welded to the prong and driven by the hydraulic pistons. The MT and DCT forks differ only in terms of prong shape.

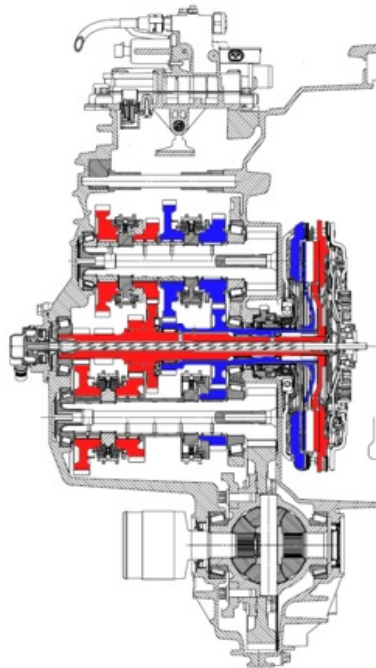


**Figure 2.5:** Cross section of the C635 DDCT

### **2.2.1 Operation of the DDCT**

The C635 DDCT is an automatically shifted transaxle, electronically controlled with a dual-clutch system for torque conversion. The most important part of the transaxle is the main shaft that is made up of two reciprocally coaxial driveshafts. The transmission of the torque to the main shaft is done employing two dry clutches, operated by two separate slave cylinders.

A basic concentric slave cylinder, placed under the gearbox casing, operates the even-number gear clutch. Another slave cylinder, located at the back of the gearbox casing, is used to operate the odd-number gear clutch. These two slave cylinders are actuated and the gears are shifted by the hydraulic power unit which is controlled by a special-purpose transmission control module.

The design of the transaxle is done in order to optimize the gear shift points, as if driving with a manual gearbox, while delivering an uninterrupted drive torque to the wheels. Another important benefit is guaranteeing smooth gear shifting that is normally associated with an automatic transmission. The C635 DDCT has the benefits of manual shifting without the complexity found in an automatic transmission.

The shift from one gear to the next one is realized as follows: when accelerating, the engine speed increases before reaching the point where the shift to the next gear should be done. If the transaxle is manual, the driver depresses the clutch pedal, moves the shift lever to the next position and finally releases the clutch. Adopting this dry dual clutch transmission, even if the clutch for the current gear remains engaged, the gears are moved to the next position by the hydraulic power unit because the clutch for the next gears is not engaged. Actually, it is a sort of preselection of the next gear before the clutch is engaged.

At the appropriate moment, the clutch for the current gear disengages and the clutch for the next gear engages. Everything is done without interrupting torque delivery to the wheels, considering that the disengagement of current gear clutch and the engagement of the next gear clutch actually overlap. In order to shift from an odd-number gear to an even-number one, it is only required that the clutches are actuated so that one engages and the other one disengages.

The hydraulic power unit represents a key part of the entire transaxle. This gives hydraulic energy for performing power-unit two functions. In primis, it selects and engages the gears in the transaxle, and then it actuates the slave cylinders that engage and disengage the clutches. The hydraulic power unit has an accumulator

very similar to the one present in the anti-locking brake system, that maintains the operating pressure (435 psi). The hydraulic power unit primes itself before the ignition is turned on, so that, when the front doors of the vehicle are open a slight pump noise can be heard.

The C635 DDCT engages each gear in a sequence; a 1-2 shift is followed by a 2-3 shift and so on. In certain conditions, the transaxle is allowed to skip gears, so that a 6-4 downshift can occur when passing a vehicle on the freeway. This ability allows a downshift of one, two or three gears, in order to meet the pedal requests of the driver.

If the vehicle increase its speed when traveling downhill with a gear engaged and the accelerator released, the clutch closes automatically, after reaching a preset speed, and provides the engine brake function. The quantity of engine braking transmitted through the clutch is usually based on the vehicle operating conditions.

### **2.2.2 Dry Dual Clutch Unit**

The analysis of the model, divided into different subsystems, is directly related to the knowledge of the different parts that make up the DDCT as it is. The torque transmission is obtained, during the shifting phase, through the engagement of the closing clutch and the release of the opening one. The position sensor, integrated in the rear-hydraulic piston actuator, controls the position of the clutch K1 that is closed as in manual transmissions. The clutch K2 is in this phase open and is controlled in force through hydraulic pressure given by the Concentric Slave Cylinder (CSC). [3] Both clutches act on a centre plate with characteristics related to the need of thermal dissipation especially during the critical phases.

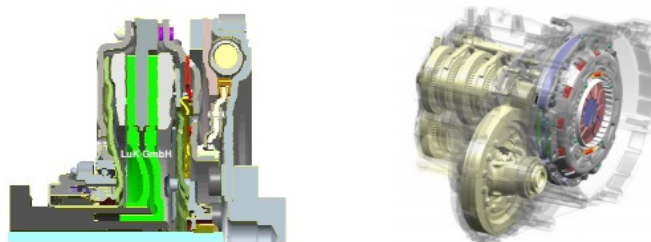


**Figure 2.6:** Dual Clutch Unit, Clutch Actuators and installation

### 2.2.3 Electro-hydraulic actuation system

The C635 DDCT clutches and gear shifting mechanisms are electro-hydraulically operated through a dedicated hydraulic oil circuit. The reason for this choice was the good system efficiency and compactness as well as Fiat Powertrain Technologies long experience with similar systems in its various Automated Manual Transmission applications. The system is composed by a hydraulic power unit (PU), consisting of an electrically driven high pressure pump and accumulator, and an Actuation Module (CAM) in which the control solenoid valves, gear shift actuators and sensors are included. The maximum operating pressure of the system under normal driving conditions does not exceed the 20 bar, even if in some particular and rare situations it can reach 39 bar. The electric oil pump is driven by a Smart Drive Unit (SDU), controlled through a Pulse Width Modulation (PWM) signal: in this way the pump speed can be regulated in order to reduce noise or to increase the efficiency. The pump's duty cycle in urban driving rarely exceeds 25% and it is a clear proof of the system's efficiency when compared to other concepts that need continuous operation of a mechanically driven hydraulic pump. This makes possible the use of a brushed motor for the pump drive.

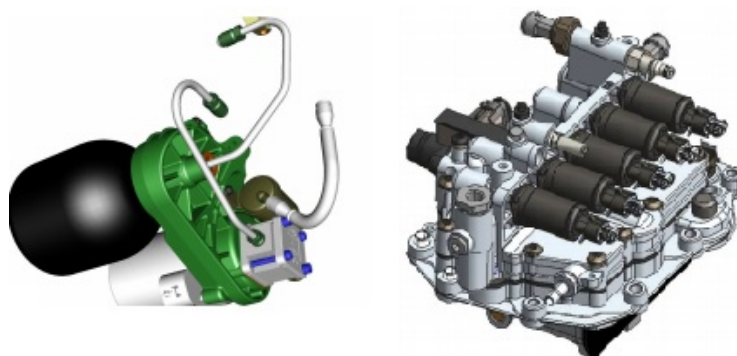


**Figure 2.7:** Hydraulic Power Unit and CAM

The clutch and gear actuation module (CAM), is made up of 4 distinct double action pistons actuating the gear engagement forks, one “shifter” spool which selects the piston to be actuated and 5 solenoid valves with 4 pressure proportional (PPV) and one flow proportional (QPV). Two of the pressure proportional valves actuate the gear engagement piston which is selected by the spool valve operated by the third PPV. The fourth PPV is used for the control of the K2 clutch. The flow proportional valve is used for the position control of the K1 clutch. The solenoid valves are directly derived by those currently used in FPT's AMT systems and, therefore, adopt well proven technologies and guarantee robustness. The Actuation Module also has 5 non-contact linear position sensors, one for each shifting piston

and one for the shifter spool, together with two speed sensors reading the speed of the two primary shafts. One pressure sensor is used for the control of the K2 clutch and one for the system pressure monitoring and control. The K1 clutch position sensor, as explained before, is integrated in the clutch piston actuator placed at the rear of the transmission. Figure below represents the hydraulic circuit of the complete actuation system (CAS).

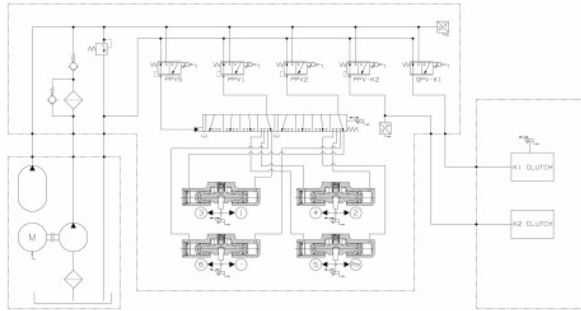


**Figure 2.8:** C635 DDCT complete actuation system

## 2.2.4 DDCT Control Unit

The C635 DDCT control strategies run in a multitasking environment so that the Main Micro Controller resources are optimally managed. These strategies can be grouped as:

- Actuator Control: exploits the high performance achievable with electro- hydraulic actuators. The main control strategies deal with:
  - Engagement Actuators Control: the desired trajectories are realized by commanding the two relevant PPVs one against the other.
  - Shifter Control: hydraulic power to the required engagement actuator is guaranteed by a fast and precise control of the shifter, obtained by commanding the related PPV to push the shifter piston against the spring in order to reach the desired position.
  - Odd Gears Clutch Control: the normally closed clutch (K1), which is the clutch of the first and of the reverse gear, is controlled by a position closed loop.

- Even Gears Clutch Control: the normally open clutch (K2) is controlled in force with a pressure feedback signal delivered by one of the CAM sensors.
- Self-Tuning Control: many self-tuning controls are needed in order to compensate for the various parameters' drift and to guarantee the same high-level calibrations to all vehicles. The main self-tuning control algorithms concern the conversion of the requested clutch transmitted torque to K1 position and K2 pressure.
- Launch and Gear Shift strategies: different modes of shift patterns in automatic and in manual mode are contemplated and are accomplished by specific control strategies and calibrations on the engine side.

## 2.3 Micro slip

The Dry Dual Clutch is made up of two different clutches K1 and K2: the first one is connected with the inner primary shaft and the odd gears, the second one is linked with the outer primary shaft and the even gears. The center plate has two different contact surfaces where the sliding problem is located.

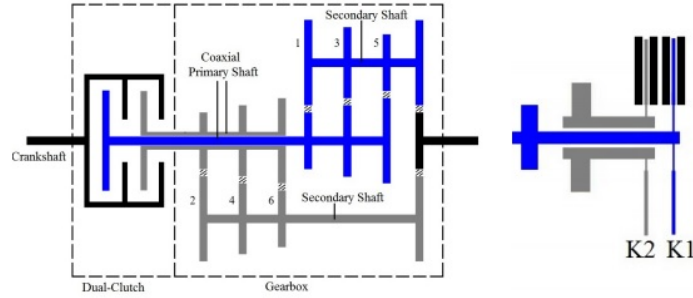


**Figure 2.9:** DCT and clutches K1 and K2

The micro-slip problem affects both clutches at different times, so in this work the design of the controller is referred only to one of the clutches. The clutch is essentially composed by two rotating friction surfaces that are pressed against each other by a normal force  $F_n$ .

The presence of friction at the contact surface realizes the transmission of the clutch torque  $C_f$ . The effective torque that can be transmitted depends on the value of  $F_n$ .

In the following Figure 2.10 it is possible to see a schematic representation of the DDCT including the engine torque  $C_m$  and the torque given by the reaction of the driveline  $C_r$ , the angular speeds are also represented ( $\omega_m, \omega_p$ ).

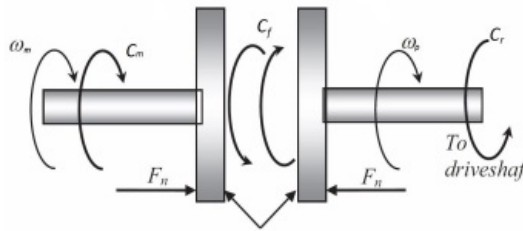


**Figure 2.10:** Schematic representation of the DDCT

The three different phases in which the clutch can be in ordinary operating conditions can be the following ones:

-Open clutch phase: the two disks are completely disengaged  $C_f = 0$ ;

-Slipping phase: the difference between the engine speed and the primary shaft speed is not zero  $\omega_d = \omega_m - \omega_p$ ;

-Closed clutch phase: the synchronization of the engine shaft and the primary shaft is completed and the torque is fully transmitted  $C_f = C_m$ .

The micro-slip effect is related to the slipping phase and the objective of the control design studied in this thesis is to guarantee a smooth slip between the clutch disks. The control determines a better engagement of the clutch reducing driveline oscillations and jerks and allowing a partial decoupling from the high dynamics of the engine to obtain a better driving comfort.

The aim is that to design a feedback controller using the Linear Quadratic Integral control in order to make the slipping speed  $\omega_d$  to track a given reference signal. Another control target is that to bring  $\omega_{sr}$  that is the torsion velocity of the transmission to zero.

## 2.4 State of art

The dry dual clutch engagement together with the micro-slip problem have been already analysed in literature and different solutions have been developed in order to realize the clutch slipping control and the reduction of torque oscillations.

In [4] a control with two independent PID controllers P1 and P2 is presented: the engine speed  $\omega_e$  and the slipping speed are tracked independently as shown in the figure below:

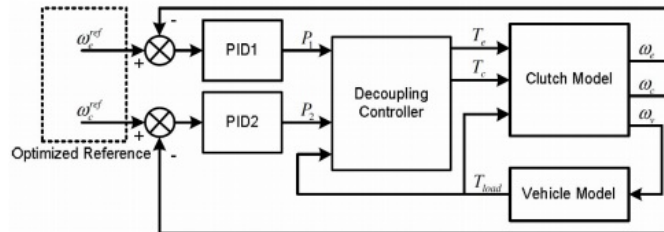


**Figure 2.11:** Decoupling control implemented in [4]

The system represents a two input and two output decoupled control.

Both models, the clutch and the vehicle ones, provide a feedback in terms of speed in order to guarantee a smooth clutch engagement and a better reference tracking.

Another control is proposed in [5]: only the clutch torque is here used as a control variable and the engine torque is considered a non- controllable signal. The engine torque is subjected to a lot of constraints that are the result of a trade-off between fuel efficiency, emissions and traction control. These constraints do not allow to adoperate the engine torque as a control variable.

The throttle pedal position  $x_p$  determines the output engine torque given by the ECU, engine control unit, that is used by the vehicle model in order to compute the angular velocity  $\omega_e$  and  $x_0$ .

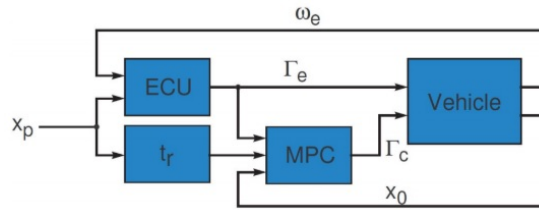


**Figure 2.12:** MPC control from [5]

The total engagement time  $t_f$ , that is computed in function of the throttle pedal position, is used to calculate the time control horizon  $t_r$ . The clutch torque is then computed throught the MPC control strategy solving the optimal control problem with a suitable cost function.

In [6], in order to prevent undesirable effects about non linearities and saturation, a torque rate limitation strategy is implemented for the gearshift control. The controlled clutch is actuated only in one direction: the oncoming clutch normal force can be only increased or held, while the off-going clutch normal force can be decreased or held. By measurements of the two clutches engine speeds, the target engine speed is computed and the engine torque controller is implemented as a proportional-integrative PI. The engine torque is controlled also by the feedback of the speed tracking error.

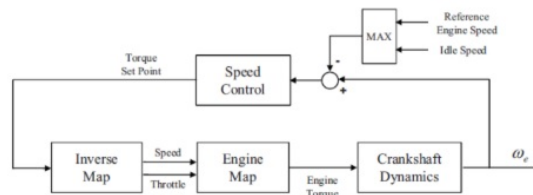


**Figure 2.13:** Engine speed and torque control [6]

In article[7] the author suggests a controller based on the different five AMT operating conditions: engagement, slipping opening, synchronization, go to slip and slipping closing. In this case the measurement of engine speed, clutch speed and the estimation of the transmitted torque give the possibility to realize decoupled and cascade feedback loops. In this case the control target is that to reach the engagement phase in a short amount of time avoiding the engine stall.

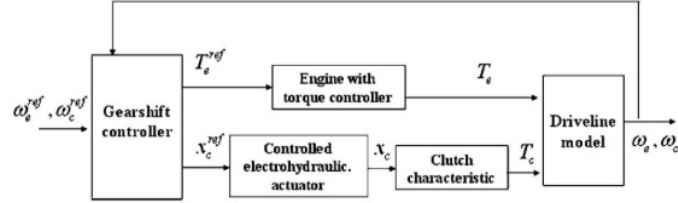


Figure 2.14: General scheme presented in [7]

## 2.5 Model configuration

In order to describe the model into details it is necessary to analyze all the elements connected to the Dry Dual Clutch used by Centro di Ricerche Fiat.

In the Figure below, a general scheme of the model is presented with the following components:

- the engine that gives the torque  $C_m$ ;
- the torque  $C_{Load}$  that includes the effects of the air;
- the reference generator that gives the reference angular speed  $\omega_{ref}$  for the clutch slipping speed  $\omega_d$ ;
- the actuator of the clutch torque  $C_f$  given by the controller;
- DDCT system that includes the clutch and the transmission.

All these elements are described in details and their implementation in Matlab Simulink environment is shown.

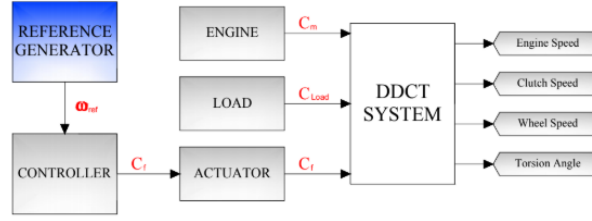


**Figure 2.15:** Overall model of the DDCT system

### 2.5.1 Actuators

The actuators are an important part of the system because they allow the transmission of the two torques  $C_m$  and  $C_f$ :

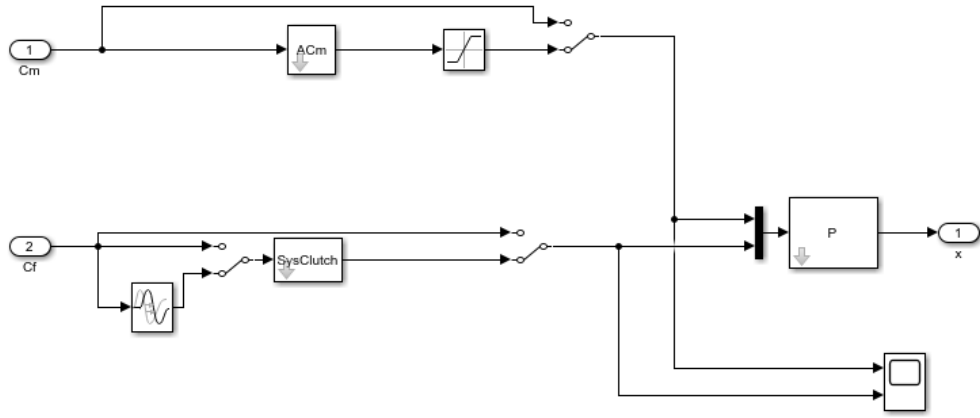


**Figure 2.16:** Actuators for  $C_m$  and  $C_f$

The actuator block  $AC_m(s)$  contains the transfer function for the engine torque actuator that is:

$$AC_m(s) = e^{-0.02 \cdot s} \cdot \frac{14.05}{s + 14.15} \quad (2.1)$$

The block  $SysClutch(s)$  represents the behavior of the actuator that realizes the requested value of the transmitted torque  $C_f$ :

$$SysClutch(s) = \frac{25.305(s + 138)(s^2 - 161.3s + 161.3s + 3.134 \cdot 10^4)}{(s^2 - 82.23s + 2563)(s^2 - 134.1s + 4.27 \cdot 10^4)} \quad (2.2)$$

A delay block is also present (*ActuatorDelay*) with a delay of 20 ms.

## 2.5.2 Engine model

In this section the model of the engine is presented. This input of the plant is computed by the LQI controller through the  $\omega_{ref}$  that has the following behavior:

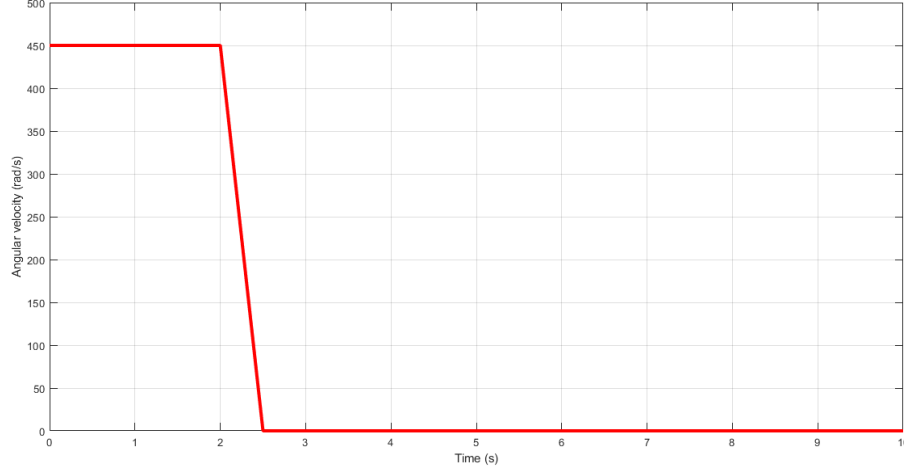


**Figure 2.17:** Reference angular velocity

The state-feedback control is of the form

$$u = -k[x; x_i] \quad (2.3)$$

where  $x_i$  is the integrator output and  $u$  is given by the two torques  $C_m$  and  $C_f$ .

## 2.5.3 Load

The load contribution is given by three different terms:

- Aerodynamic resistance force:

$$F_a = 0.5\rho_a A_f C_a (v_a + v_v)^2 \quad (2.4)$$

Where:

- $\rho_a$  is the air density;
- $A_f$  is the frontal area of the vehicle;
- $C_a$  is the aerodynamic drag coefficient;
- $v_a$  is the wind speed;

-  $v_v$  is the vehicle speed.

- Rolling resistance force:

$$F_r = m_v g \mu_r \cos(\beta) \quad (2.5)$$

With the following terms:

- $m_v$  is the vehicle mass;
- $g$  is the gravity acceleration;
- $\mu_r$  is the rolling friction coefficient;
- $\beta$  is the slope of the road.

- Uphill driving force: resistance force when driving on a non-horizontal surface. It is given by:

$$F_g = m_v g \sin(\alpha) \quad (2.6)$$

The final expression of the total load torque, considering the wheel radius  $r_w$  is:

$$C_{Load} = (F_a + F_r + F_g)r_w \quad (2.7)$$

## **2.6 Hybrid electric vehicles with P2 architecture**

This section is focused on the explication of the implementation of the parallel hybrid vehicle model.

Accordingly to the analyzes carried out by Yalian Yang researchers, Xiaosong Hua, Huanxin Pei, Zhiyuan Peng reported in the scientific article "Comparison of power-split and parallel hybrid powertrain architectures with a single electric machine: Dynamic programming approach ", among the various parallel architecture, the P2 is advantageous in terms of fuel saving with respect to the P1 architecture.

The parallel hybrid vehicle is characterized by having a thermal engine and an electric motor constrained to the wheels, the power and torque provided for the propulsion is the result of an excellent contribution of both.

Unlike other hybrids, it only requires a single motor, a standard transmission and two clutches. This clutch is used to operate the gas engine and the electric motor separately without the need for two separate engines. This is where the cost saving comes in.

With the P2 technology, the cost can be reduced by more than one-thirds. While P2 hybrid cars have clear advantages, they also face a problem when starting the engine when running down the road in electric mode. Different car manufacturers are trying to find ways to solve this problem.

The fuel efficient hybrid cars have surely secured a place for the richer class of people but its high price has kept the hybrids far from the reach of most new car buyers. The P2 technology is sure to bring its price down and make the hybrids affordable enough for widespread use.

Key advantages include:

- The major advantage is its low cost which will open the hybrid market for all customers.
- The P2 system gives better regenerative braking.
- The P2 technology does not require a torque converter and hence its cost is reduced further.
- They use high power lithium-ion batteries which are smaller, lighter and have a low cost.
- Vehicle Load is reduced by using only single motor and other lighter parts.

Some key limitations of P2 Hybrids are related to:

- Inability to start the engine while running on electric mode only.
- The driving may not be as smooth with the manual transmission and their might be more wear and tear because of the complex gear system.

# Chapter 3

## Model Analytical description

### 3.1 Introduction

In order to design a Linear Quadratic Integral controller LQI, together with the other techniques needed in order to compensate the delays and non-linearities of the system, the computation of the state-space model is needed. The general driveline scheme, that is a linear model, gives a good representation of the system that is essentially made up of: the engine, the crankshaft, the clutch, the main shaft, the gearbox, the secondary shaft, the differential and the wheel shaft.

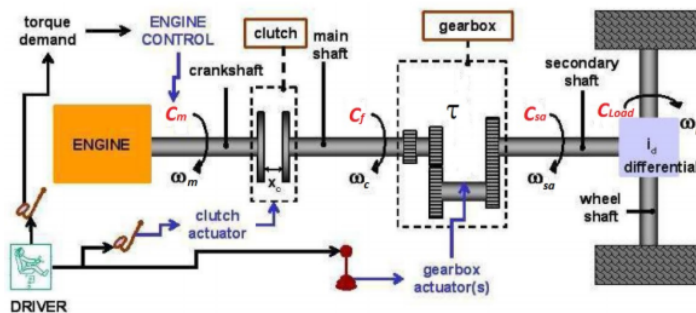


Figure 3.1: General driveline scheme

From this basic scheme it is possible to derive the specific DDCT driveline scheme where it is possible to observe the odd gears and the even ones.

In order to derive the linear model of the driveline three assumptions are made:

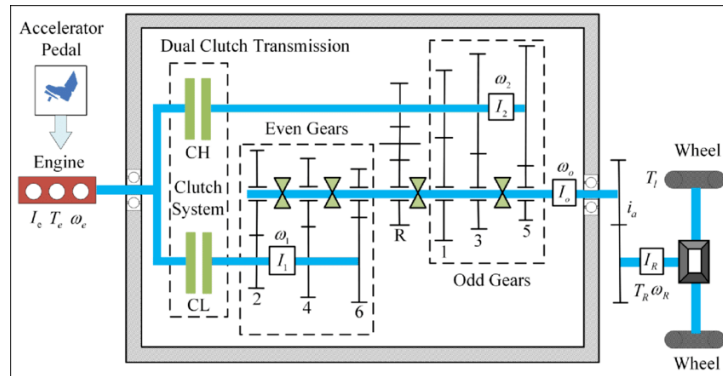


Figure 3.2: DDCCT driveline scheme

- 1) The main shaft is perfectly rigid;
- 2) The wheels motion is pure rolling;
- 3) The two branches of the driveline are perfectly simmetric.

Starting from these considerations, the following scheme of the driveline can be built, considering linear conditions:

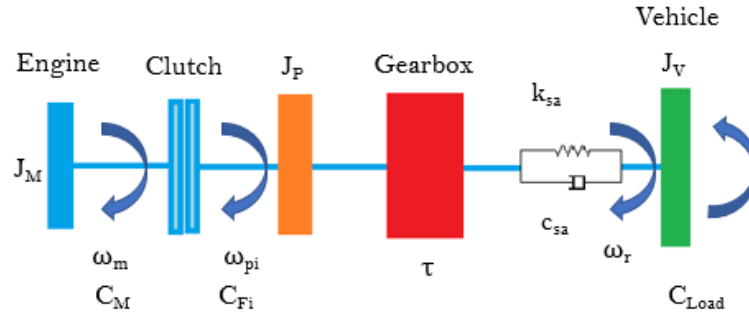


Figure 3.3: Reduced linear driveline scheme

### 3.2 State Space representation

The values and meaning of the parameters shown in Figure 3.3 are explained in the table below:

Component	Symbol	Value
Torsional damping coefficient	$c_{sa}$	105 (Nm/(rad/s))
Torsional stiffness coefficient	$k_{sa}$	6719 (Nm/rad)
Gear ratio (second gear)	$\tau$	10.473
Wheel radius	$r_W$	0.308 (m)
Wheel inertia	$J_W$	3 (kgm <sup>2</sup> )
Vehicle mass	$M$	1550 (kg)
Vehicle inertia	$J_v$	$M \cdot r_W^2 + J_W$ (kgm <sup>2</sup> )
Motor damping coefficient	$c_m$	105 (Nm/(rad/s))
Motor inertia	$J_m$	0.28 (kgm <sup>2</sup> )

**Table 3.1:** DDCT main parameters

Imposing the rotational equilibrium for the system in Figure 3.3, the system of differential equations is obtained:

$$J_m \dot{\omega}_m = C_m - c_m \omega_m - C_f \quad (3.1)$$

$$J_p \dot{\omega}_p = C_f + \frac{1}{\tau} (-c_{sa} \omega_{sr} - k_{sa} \theta_{sr}) \quad (3.2)$$

$$J_v \dot{\omega}_r = c_{sa} \omega_{sr} + k_{sa} \theta_{sr} - C_{Load} \quad (3.3)$$

$$\dot{\theta}_{sr} = \omega_{sr} \quad (3.4)$$

With:

$$\theta_{sr} = \theta_{sa} - \theta_r \quad (3.5)$$

$$\omega_{sr} = \frac{\omega_p}{\tau} - \omega_r \quad (3.6)$$

Putting together all the equations the final form of the equations is:

$$\dot{\omega}_m = \frac{1}{J_m} (C_m - C_f) - \frac{c_m}{J_m} \omega_m \quad (3.7)$$

$$\dot{\omega}_p = \frac{C_f}{J_p} + \frac{1}{\tau J_p} \left( -\frac{c_{sa} \omega_p}{\tau} + c_{sa} \omega_r - k_{sa} \theta_{sr} \right) - \frac{C_{prim} \omega_p}{J_p} \quad (3.8)$$

$$\dot{\omega}_r = \frac{c_{sa} \omega_p}{J_v \tau} - \frac{c_{sa} \omega_r}{J_v} + \frac{k_{sa} \theta_{sr}}{J_v} - \frac{C_{Load}}{J_v} \quad (3.9)$$

$$\dot{\theta}_{sr} = \frac{\omega_p}{\tau} - \omega_r \quad (3.10)$$

In order to build through these last equations the state space representation, the input vector, the output vector and states have to be defined:

- The input vector is  $u(t) = [C_m(t), C_f(t), C_{Load}(t)]^T$
- The state vector is  $x(t) = [\omega_m(t), \omega_p(t), \omega_r(t), \theta_{sr}(t)]^T$
- The output vector is  $y(t) = [\omega_d(t), \omega_{sr}(t)]^T$  where  $\omega_d(t) = \omega_m(t) - \omega_p(t)$  is the slipping velocity and  $\omega_{sr}(t) = \frac{\omega_p(t)}{\tau} - \omega_r(t)$  is the torsion speed.

Considering the general state space representation:

$$\dot{x}(t) = Ax(t) + Bu(t)$$

$$y(t) = Cx(t) + Du(t)$$

with:

$$A = \begin{bmatrix} -\frac{c_m}{J_m} & 0 & 0 & 0 \\ 0 & -\left(\frac{c_{sa}}{J_p\tau^2} + \frac{c_{prim}}{J_p}\right) & \frac{c_{sa}}{J_p\tau} & -\frac{k_{sa}}{J_p\tau} \\ 0 & \frac{c_{sa}}{J_v\tau} & -\frac{c_{sa}}{J_v} & \frac{k_{sa}}{J_v} \\ 0 & \frac{1}{\tau} & -1 & 0 \end{bmatrix} \quad (3.11)$$

$$B = \begin{bmatrix} \frac{1}{J_m} & -\frac{1}{J_m} & 0 \\ 0 & \frac{1}{J_p} & 0 \\ 0 & 0 & -\frac{1}{J_v} \\ 0 & 0 & 0 \end{bmatrix} \quad (3.12)$$

$$C = \begin{bmatrix} 1 & -1 & 0 & 0 \\ 0 & \frac{1}{\tau} & -1 & 0 \end{bmatrix} \quad (3.13)$$

$$D = \begin{bmatrix} 0 & 0 & 0 \\ 0 & 0 & 0 \end{bmatrix} \quad (3.14)$$

In order to change the states vector to  $x(t) = [\omega_m(t), \omega_m(t) - \omega_p(t), \frac{\omega_p(t)}{\tau} - \omega_r(t), \theta_{sr}(t)]^T$  with  $\omega_d(t) = \omega_m(t) - \omega_p(t)$  and  $\omega_{sr}(t) = \frac{\omega_p(t)}{\tau} - \omega_r(t)$  the following transformation matrix  $T_x$  is involved:

$$T_x = \begin{bmatrix} 1 & 0 & 0 & 0 \\ 1 & -1 & 0 & 0 \\ 0 & \frac{1}{\tau} & -1 & 0 \\ 0 & 0 & 0 & 1 \end{bmatrix} \quad (3.15)$$

And the matrices become:

$$A' = T_x A T_x^{-1}$$

$$B' = T_x B$$

$$\text{with } C' = \begin{bmatrix} 1 & 0 & 0 & 0 \\ 0 & 1 & 0 & 0 \\ 0 & 0 & 1 & 0 \\ 0 & 0 & 0 & 1 \end{bmatrix} \text{ choosing the outputs equal to the states.}$$

### 3.3 Complete model with actuators

In this section the full implementation of the model is explained where both the engine and the clutch actuators are considered. The final form of the state space representation used in order to implement the Kalman observer together with the LQI controller is here computed.

From the transfer functions of the actuators, built in Simulink, a linearized state space model is derived.

For the clutch actuator the general state space equations are:

$$\dot{z}(t) = Fz(t) + Gv(t)$$

$$u(t) = Hz(t)$$

And for the engine actuator:

$$\dot{g}(t) = Lg(t) + Mr(t)$$

$$u'(t) = Ng(t)$$

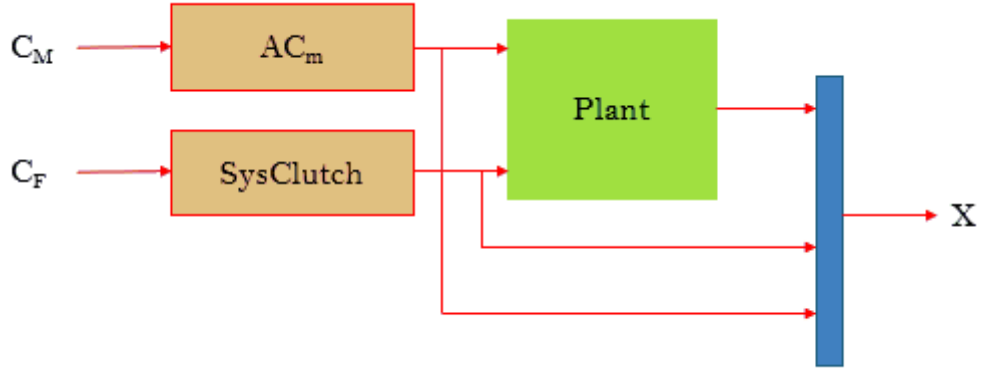


**Figure 3.4:** Complete model with actuators

At this point a new complete state space representation can be built with 9 states, where the states determined by the actuators transfer functions need to be predicted in order to control the system.

$$X = \begin{bmatrix} x \\ z \\ g \end{bmatrix} \quad U = \begin{bmatrix} v \\ r \end{bmatrix}$$

$$\begin{bmatrix} \dot{x} \\ \dot{z} \\ \dot{g} \end{bmatrix} = \begin{bmatrix} A & B(:,2)H & B(:,1)N \\ \text{zeros}(4,4) & F & \text{zeros}(4,1) \\ \text{zeros}(1,4) & \text{zeros}(1,4) & L \end{bmatrix} \begin{bmatrix} x_1 \\ \dots \\ x_n \\ z_1 \\ \dots \\ z_n \\ g \end{bmatrix} + \begin{bmatrix} \text{zeros}(4,1) & \text{zeros}(4,1) \\ G & \text{zeros}(4,1) \\ 0 & M \end{bmatrix} \begin{bmatrix} v \\ r \end{bmatrix}$$

$$\dot{X}(t) = \bar{A}X(t) + \bar{B}U(t)$$

The matrices concerning the state space models for the actuators are computed by Simulink using the command "Linmod". This complete model is used in order to improve the performance of the LQI control associating it with other techniques in order to guarantee an optimal management of the actuators effects and the delays related to them.

The starting model taken into consideration is realized without actuators and delays in order to verify the performance of the controller in the initial conditions. The following techniques are then associated to the LQI controller to compensate the delays of the real model:

- LQI technique with and without the delay of the clutch actuator;
- LQI linearization of the entire nonlinear model and actuator delay;
- LQI control with Smith Predictor;
- State space representation of the actuators and the Plant with LQI technique;
- State space representation of the actuators and the Plant with LQI technique and Kalman observer.

# Chapter 4

## LQI technique

### 4.1 Linear Quadratic regulator

The optimal control theory is related to operating a dynamic system at minimum cost. The situation where the system dynamics are represented by a set of linear differential equations and the cost is described by a quadratic function is referred to the LQ problem. In this case, one of the main results in the theory is that the solution is provided by the linear-quadratic regulator (LQR), a feedback controller whose equations are given below.

The LQR algorithm is essentially an automated way of finding an appropriate state-feedback controller.

#### 4.1.1 Finite-horizon, continuous-time LQR

The finite horizon, linear quadratic regulator (LQR) for a continuous-time linear system defined on  $t \in [t_0, t_1]$  is given by [8]:

$$\dot{x} = Ax + Bu \quad (4.1)$$

$$J = x^T(t_1)F(t_1)x(t_1) + \int_{t_0}^{t_1} (x^T Qx + u^T Ru + 2x^T Nu) dt \quad (4.2)$$

The feedback control law that minimizes the value of the cost is:

$$u = -Kx \text{ with } K = R^{-1}(B^T P(t) + N^T) \quad (4.3)$$

P is then found by solving the continuous time Riccati differential equation:

$$A^T P(t) + P(t)A - (P(t)B + N)R^{-1}(B^T P(t) + N^T) + Q = -\dot{P}(t) \quad (4.4)$$

with the boundary condition:  $P(t_1) = F(t_1)$ .

The first order conditions to find  $J_{min}$  are:

- State equation :  $\dot{x} = Ax + Bu$
- Co-state equation:  $-\dot{\lambda} = Qx + Nu + A^t\lambda$
- Stationary equation:  $0 = Ru + N^T x + B^T \lambda$
- Boundary conditions:  $x(t_0) = x_0$  and  $\lambda(t_1) = F(t_1)x(t_1)$

### 4.1.2 Infinite-horizon, continuous-time LQR

For a continuous-time linear system described by:

$$\dot{x} = Ax + Bu \tag{4.5}$$

with a cost function defined as:

$$J = \int_0^\infty (x^T Q x + u^T R u + 2x^T N u) dt \tag{4.6}$$

The feedback control law that minimizes the value of the cost is:

$$u = -Kx \text{ with } K = R^{-1}(B^T P + N^T) \tag{4.7}$$

P is then found by solving the continuous time algebraic Riccati equation:

$$A^T P + P A - (P B + N) R^{-1} (B^T P + N^T) + Q = 0 \tag{4.8}$$

### 4.1.3 Finite-horizon, discrete-time LQR

For a discrete-time linear system described by:

$$x_{k+1} = Ax_k + Bu_k \tag{4.9}$$

with a performance index defined as:

$$J = x_N^T Q x_N + \sum_{k=0}^{N-1} (x_k^T Q x_k + u_k^T R u_k + 2x_k^T N u_k) \tag{4.10}$$

the optimal control sequence minimizing the performance index is given by:

$$u_k = -F_k x_k \text{ with } F_k = (R + B^T P_{k+1} B)^{-1} (B^T P_{k+1} A + N^T) \quad (4.11)$$

and  $P_k$  is found iteratively backwards in time by the dynamic Riccati equation:

$$P_{k-1} = A^T P_k A - (A^T P_k B + N)(R + B^T P_k B)^{-1} (B^T P_k A + N^T) + Q \quad (4.12)$$

from terminal condition  $P_N = Q$ .

Consider that  $u_N$  is not defined, since  $x$  is driven to its final state  $x_N$  by  $Ax_{N-1} + Bu_{N-1}$ .

#### 4.1.4 Infinite-horizon, discrete-time LQR

For a discrete-time linear system described by:

$$x_{k+1} = Ax_k + Bu_k \quad (4.13)$$

with a performance index defined as:

$$J = \sum_{k=0}^{\infty} (x_k^T Q x_k + u_k^T R u_k + 2x_k^T N u_k) \quad (4.14)$$

the optimal control sequence minimizing the performance index is given by:

$$u_k = -F x_k \text{ with } F = (R + B^T P B)^{-1} (B^T P A + N^T) \quad (4.15)$$

and  $P$  is the unique positive definite solution to the discrete time algebraic Riccati equation (DARE):

$$P = A^T P A - (A^T P B + N)(R + B^T P B)^{-1} (B^T P A + N^T) + Q \quad (4.16)$$

One of the ways to solve the algebraic Riccati equation is by iterating the dynamic Riccati equation of the finite-horizon case until it converges.

## 4.2 Incorporating integral action in LQR

The LQR control law fundamentally gives a multivariable proportional regulator. An integral action has been incorporated in the LQR controller by augmenting system with error in the state variable. One new state is added to the space model of the system. In this way a Linear Quadratic Integral control is obtained with the following general scheme:

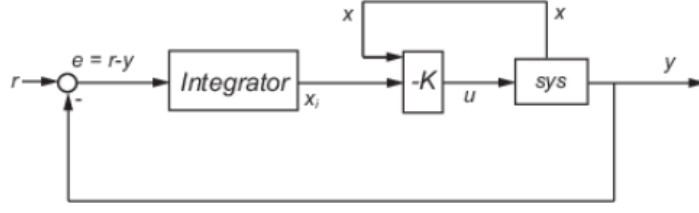


**Figure 4.1:** General LQI scheme

In order to obtain steady state zero tracking error it is possible to introduce, within the system equations, the information of the discrete time integral of the tracking error:

$$q(k+1) = q(k) + T(r(k) - y(k)) = q(k) + Te(k) \quad (4.17)$$

And considering the SISO case, by adding to the system state the discrete time integral of the tracking error an augmented state is introduced:

$$x_{tot} = \begin{bmatrix} q(k) \\ x(k) \end{bmatrix} \in R^{n+1} \quad q(k) \in R \quad (4.18)$$

The system equations become:

$$x_{tot}(k+1) = \begin{bmatrix} q(k+1) \\ x(k+1) \end{bmatrix} = \begin{bmatrix} 1_{1 \times 1} & -TC \\ 0_{n \times 1} & A \end{bmatrix} \begin{bmatrix} q(k) \\ x(k) \end{bmatrix} + \begin{bmatrix} 0 \\ B \end{bmatrix} u(k) + \begin{bmatrix} T \\ 0 \end{bmatrix} r(k) \quad (4.19)$$

$$y_k = \begin{bmatrix} 0_k & C \end{bmatrix} \begin{bmatrix} q(k) \\ x(k) \end{bmatrix} \quad (4.20)$$

With the new matrices  $A_{tot}$ ,  $B_{tot}$ ,  $C_{tot}$ . The augmented system is reachable if the original one is.

The selected control law is modified as:

$$u(k) = -Kx_{tot}(k) \text{ with } K = \begin{bmatrix} K_i & K_o \end{bmatrix} \in R^{n+1} \quad (4.21)$$

$$u(k) = - \begin{bmatrix} K_i & K_o \end{bmatrix} \begin{bmatrix} q(k+1) \\ x(k+1) \end{bmatrix} \quad (4.22)$$

The system guarantees zero steady state tracking error when  $r(k)$  is constant. Since the feedback law guarantees asymptotic stability, at steady state  $x_{tot}(k)$  will reach constant value. Since  $x_i(k)$  is the integral of the tracking error, the equilibrium should be for  $e(k) = 0$ , thus at steady state  $r(k) = y(k)$ .

Finally the design of a LQ state feedback control law with the integral state is

performed as the canonical case, using as system matrices  $A_{tot}$ ,  $B_{tot}$ .

In Matlab the following syntax is used  $[K, S, e] = lqi(SYS, Q, R, N)$  where S is the solution of the Riccati equation and K is the optimal gain matrix with a state-space model SYS for the plant and weighting matrices Q, R, N.

The problem data must satisfy:

- The pair  $A_{tot}, B_{tot}$  is stabilizable;
- $R > 0$  and  $Q - NR^{-1}N^T \geq 0$ ;
- $(Q - NR^{-1}N^T, A_{tot} - B_{tot}R^{-1}N^T)$  has no unobservable mode on the imaginary axis (or unit circle in discrete time).

In this specific case a simplified transmission model has been used, with clutch actuator, dynamic engine model and elasticity of transmission trees. A MIMO control architecture project with LQI technique with trajectory feedback (reference – state variable) is here adopted:

- o Controls: engine torque and clutch torque;
- o State variables to adjust: difference in engine-primary speed, derivative of engine-primary speed difference, semi-axis twisting speed, semi-axis twist angle, actuators' state variables.
- o Project Plant has as equivalent state variables the difference in engine-primary speed, angle and twisting speed of the semi-axes.
- o Control objective: get a great compromise between the pursuit of the engine-primary delta reference and the vehicle driveability.
- o Uncertainties to consider: clutch and engine implementation delays, clutch transmission, engine implementation, vehicle mass, semi-axis twist elasticity.
- o Evaluate the use of a predictor (backing of the predicted variables) for optimal management of implementation delays.
- o Evaluate a state observer development to estimate unmeasured states (actuators states).
- o 10ms control discretization and performance loss assessment between continuous and discrete control.

The general architecture used for the control is the following one:

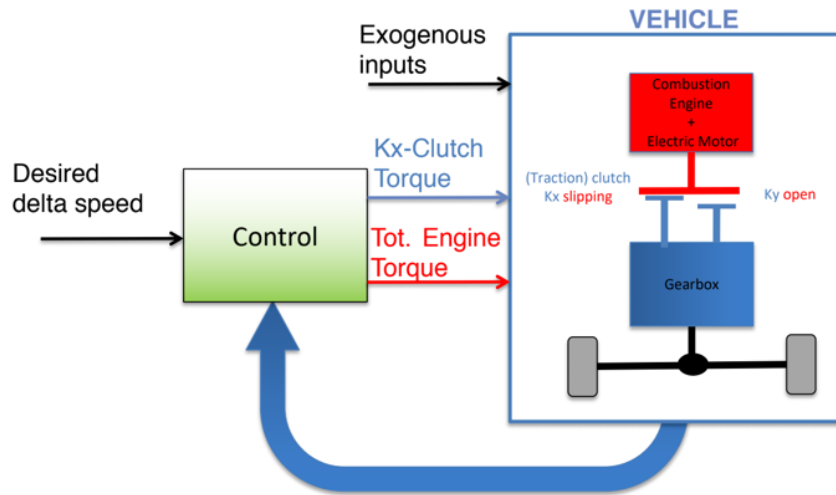


Figure 4.2: General architecture for the control

### 4.3 Optimal management of the delays

The main activity of this thesis project, realized in collaboration with CRF (Centro Ricerche Fiat), consists in developing innovative feedback control algorithms for hybrid and electric vehicles, related in particular to the control of the dual clutch transmission during its slipping phase. In this regard, the gear shifting phase is relevant because the clutch disks, when closing, do not get immediately the same angular velocity: the main control target is that of making possible a smooth convergence to zero of the difference between the combustion engine and electric motor speeds (delta speed). One of the problems related to the realization of an optimal control is the management of the delays of the actuators that creates some difficulties in the tuning of the Q and R matrices of the LQI controller. In order to solve these difficulties, different control strategies are here developed in order to realize an optimal management of the delays.

The main control strategies developed are the following ones:

-LQI technique with and without the delay of the clutch actuator;

- LQI linearization of the entire nonlinear model and actuator delays;
- LQI control with Smith Predictor;
- State space representation of the actuators and the Plant with LQI technique;
- State space representation of the actuators and the Plant with LQI technique and Kalman observer.

### 4.3.1 Smith Predictor

The field of interest is the control of systems with delays. Feedback control has several familiar advantages - one important one is the decreased sensitivity of a closed-loop negative feedback system to variations in its parameters.

The Smith predictor is a model-based controller that is effective for processes with long dead time. It has an inner loop with a main controller that can be simply designed without the dead time. The effects of load disturbance and modeling error are corrected through an outer loop. The Smith predictor can also be used for processes with significant non-minimum phase dynamics and for high order systems that exhibit apparent dead time.

Smith's predictor is a controller for dynamic systems with pure delay time dominant, i.e. in systems where delay far outweighs the time constant ( $T \gg \tau$ ). Delay is a time quantity described as the time between the effect occurs and that effect is taken into account to change the system. It is present in almost all real systems. In most analyses, a frequent error is the non-consideration of this amount, however in cases where this is presented with an irrelevant value compared to the time constant it is possible to overlook it, approximating it to a system without delays. A very high delay, on the other, creates oscillating phenomena creating problems of stability.

Smith predictor, as mentioned earlier behaves like a controller, its f.d.t. is composed of the f.d.t. of the plant  $Gp(s)$ , the delay component ( $e^{-sT}$ ) and the f.d.t. of a controller designed for the system in feedback without delay  $Gcr(s)$ . The latter controller can be designed according to the classic rules (u -Kx) or a PID, etc. [9]

The transfer function is the following one:

$$Gc(s) = \frac{Gcr(s)}{1 + Gcr(s)Gp(s)[1 - e^{-sT}]} \quad (4.23)$$

The design of a  $G_c(s)$  controller for a system whose plant is  $G_p(s)$  and there is a pure  $T$  seconds delay in the feedback loop, as shown in the following figure is such complicated:

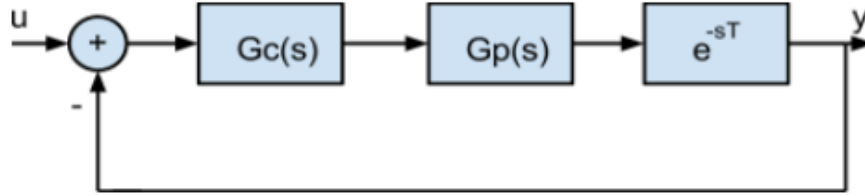


**Figure 4.3:** Controller without Smith Predictor

On the other hand, a less direct technique is that of Smith's predictor, which goes to consider a second system (as shown in the following figure) where the delay is placed outside the control ring allowing the design of a second  $G_{cr}(s)$  controller. This one can be designed as a PID regulator, through a feedback of type  $-Kx$ , etc.

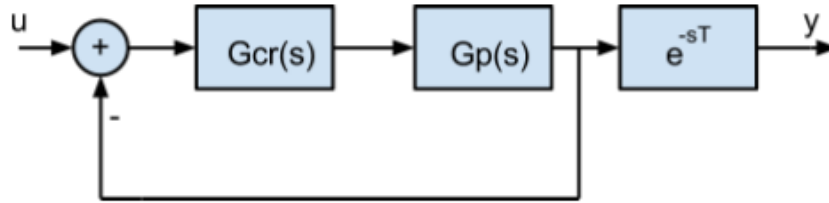


**Figure 4.4:** System considered for Smith Predictor

However, the two systems are not fully equivalent, so the design of  $G_{cr}(s)$  is not the same as designing  $G_c(s)$ . This problem is solved by equaling the two transfer functions, which is to derive the value of  $G_c(s)$  from  $G_{cr}(s)$ .

$$f.d.t.1 = \frac{G_c(s)G_p(s)e^{-sT}}{1 + G_c(s)G_p(s)e^{-sT}} \quad (4.24)$$

$$f.d.t.2 = \frac{G_{cr}(s)G_p(s)e^{-sT}}{1 + G_{cr}(s)G_p(s)} \quad (4.25)$$

$$f.d.t.1 = f.d.t.2$$

$$\frac{G_c(s)G_p(s)e^{-sT}}{1 + G_c(s)G_p(s)e^{-sT}} = \frac{G_{cr}(s)G_p(s)e^{-sT}}{1 + G_{cr}(s)G_p(s)} \quad (4.26)$$

$$\frac{Gc(s)}{1 + Gc(s)Gp(s)e^{-sT}} = \frac{Gcr(s)}{1 + Gcr(s)Gp(s)} \quad (4.27)$$

$$Gc(s) = \frac{Gcr(s)(1 + Gc(s)Gp(s)e^{-sT})}{1 + Gcr(s)Gp(s)} \quad (4.28)$$

$$Gc(s)\left(1 - \frac{Gcr(s)(1 + Gc(s)Gp(s)e^{-sT})}{1 + Gcr(s)Gp(s)}\right) = \frac{Gcr(s)}{1 + Gcr(s)Gp(s)} \quad (4.29)$$

$$Gc(s)\left(\frac{1 + Gcr(s)Gp(s) - Gcr(s)Gp(s)e^{-sT}}{1 + Gcr(s)Gp(s)}\right) = \frac{Gcr(s)}{1 + Gcr(s)Gp(s)} \quad (4.30)$$

$$Gc(s)(1 + Gcr(s)Gp(s)[1 - e^{-sT}]) = Gcr(s)$$

$$Gc(s) = \frac{Gcr(s)}{1 + Gcr(s)Gp(s)[1 - e^{-sT}]} \quad (4.31)$$

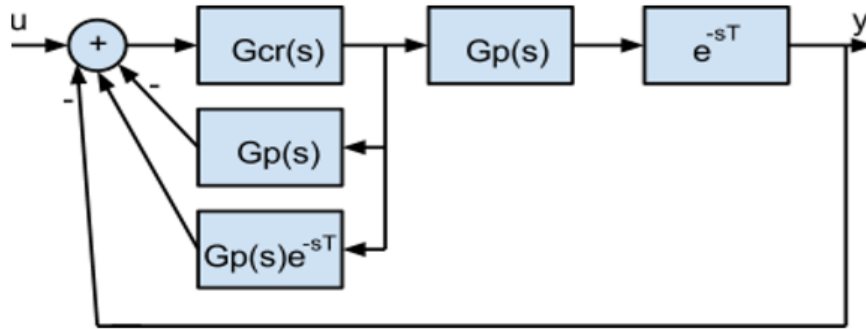
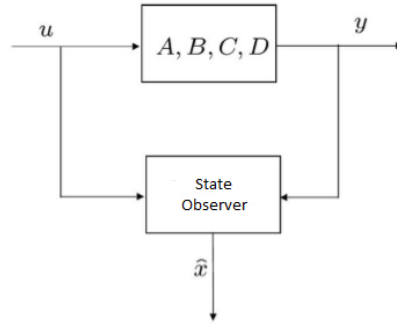


Figure 4.5: Smith Predictor

### 4.3.2 Kalman state observer

In the theoretical analysis so far, the state is always been supposed to be measured. In some cases this could not be possible and a state observer (SO) is needed in order to provide an estimate  $\hat{x}(k)$  of the system states  $x(k)$ . The estimation is generally based on the input/output measurements of the system to be controlled. The general structure of an observer is reported below:



**Figure 4.6:** General observer scheme

In statistics and control theory, Kalman filtering, also known as linear quadratic estimation (LQE), is an algorithm that uses a series of measurements observed over time, containing statistical noise and other inaccuracies, and produces estimates of unknown variables that tend to be more accurate than those based on a single measurement alone, by estimating a joint probability distribution over the variables for each time frame.

In order to design a Kalman filter, the following hypotheses are introduced: [10]

- the initial state  $x_0$  is a Gaussian variable such that:

$$E[x_0] = 0$$

$$E[x_0 x_0^T] = X_0$$

$$X_0 \geq 0$$

where  $E[ \ ]$  indicates the expected value.

- the process disturbance  $w(k)$  and the measurement error  $v(k)$  are white noises with zero mean value and known variance which are uncorrelated with each other:

$$E[w(k)] = 0, \quad E[v(k)] = 0$$

$$E[w(k)w(k)^T] = w\tilde{Q}, \quad E[v(k)v(k)^T] = v\tilde{R}$$

$$E[v(k)w(k)^T] = E[x_0 v(k)^T] = E[x_0 w(k)^T] = 0$$

The covariance matrix of the error is defined as:

$$\tilde{P}(k|k-1) = E[e_e(k|k-1)e_e(k|k-1)^T] \text{ and } \tilde{P}(0|-1) = \tilde{P}_0 \quad (4.32)$$

The gain observer  $L$  is determined by minimizing a quadratic expression of the error covariance:

$$\min_L (\psi^T \tilde{P}(k+1|k)\psi) \quad (4.33)$$

where  $\psi$  is a generic vector.

The gain  $L$  derives from the solution to the previous minimization problem:

$$L = A\tilde{P}(k|k-1)C^T + [C\tilde{P}(k|k-1)C^T + \tilde{R}]^{-1} \quad (4.34)$$

The expression  $\tilde{P}(k|k-1)$  comes from the solution of the Difference Riccati Equation (DRE):

$$\tilde{P}(k+1|k) = A\tilde{P}(k|k-1)A^T + \tilde{Q} - A\tilde{P}C^T[C\tilde{P}(k|k-1)C^T + \tilde{R}]^{-1}C\tilde{P}A^T \quad (4.35)$$

$\tilde{Q}$  and  $\tilde{R}$  are weight matrices that can be conveniently made.

The matrices  $\tilde{Q}$  and  $\tilde{R}$  are related to the information regarding the noise. The  $\tilde{R}$  diagonal elements are given by the variance of the output errors. The definition of  $\tilde{Q}$  is more complicated because the process disturbances are often unknown. Therefore, more frequently the matrices  $\tilde{Q}$  and  $\tilde{R}$  are considered as two project parameters.

## 4.4 LQI in Simulink

Matlab provides Simulink blocks for simulations. In this way it is possible to adjust the behaviour of the controller by varying its weights and constraints at run time. In this thesis the controller is designed as follows:

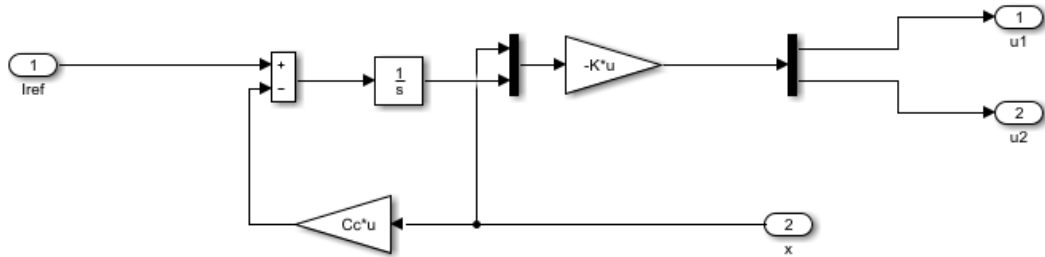


Figure 4.7: LQI controller scheme

The controller computes an optimal state-feedback control law for the tracking loop shown above.

Different blocks can be recognized:

- The reference input that is a reference signal for the delta speed  $\omega_d = \omega_m - \omega_p$ ;
- The vector of the states that in general is:  $x(t) = [\omega_m(t), \omega_m(t) - \omega_p(t), \frac{\omega_p(t)}{\tau} - \omega_r(t), \theta_{sr}(t)]^T$  even if in the full model the states of the actuators are added;
- The two inputs of the model  $u_1$  and  $u_2$  that are the engine torque and the clutch torque;
- The gain  $K$  given by the controller implementation through the Matlab command *lqi*.

## 4.5 Plant without actuators and delays

In a first approach the LQI technique is taken into account without considering the non-linearities introduced by the transfer functions of the actuators. The simplified plant model is considered with four states  $x(t) = [\omega_m(t), \omega_m(t) - \omega_p(t), \frac{\omega_p(t)}{\tau} - \omega_r(t), \theta_{sr}(t)]^T$ .

Tuning LQ regulators implies choosing the weight matrices  $Q$  and  $R$  involving some kind of trial and error procedure.

These matrices are chosen as diagonal matrices so that for a system with  $n$  states and  $p$  controls,  $n+p$  parameters have to be defined.

The diagonal values  $q_{jj}$  and  $r_{jj}$  of  $Q$  and  $R$  respectively are chosen according to the relative importance of each state and control variable, bearing in mind that  $q_{jj} \geq 0$  and  $r_{jj} > 0$ .

In principle, a first choice of the diagonal elements of  $Q$  and  $R$  is performed so that all the state and input components values appear in the cost function with almost the same order of magnitude.

After this first iteration, values are modified to impose the desired performance. Anyway the important aspect is the relative value of a single weighting coefficient with respect to the others.

The scheme of the plant and the general scheme including the controller are shown below together with the main results concerning the convergence of the delta speed  $\omega_d$  and the drive shaft torsion speed and angle  $\omega_{sr}$  and  $\theta_{sr}$ .

The control can be discretized at  $T=10$  ms in order to verify if it implies a loss of performance, that in this case remains more or less the same.

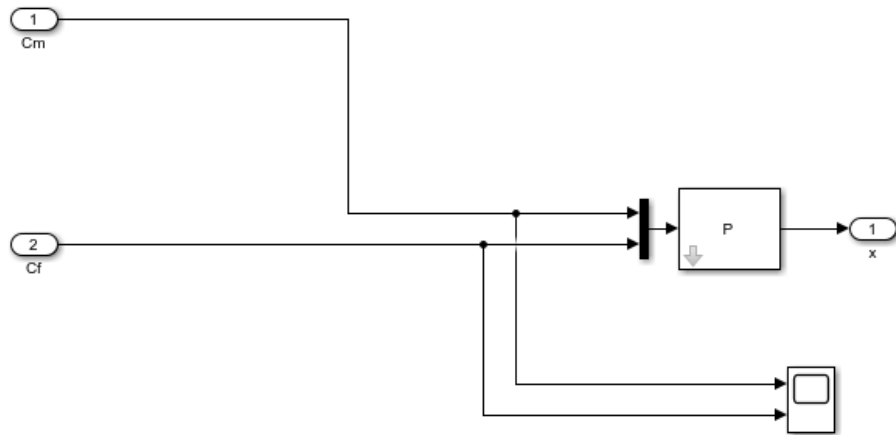


Figure 4.8: Plant without actuators

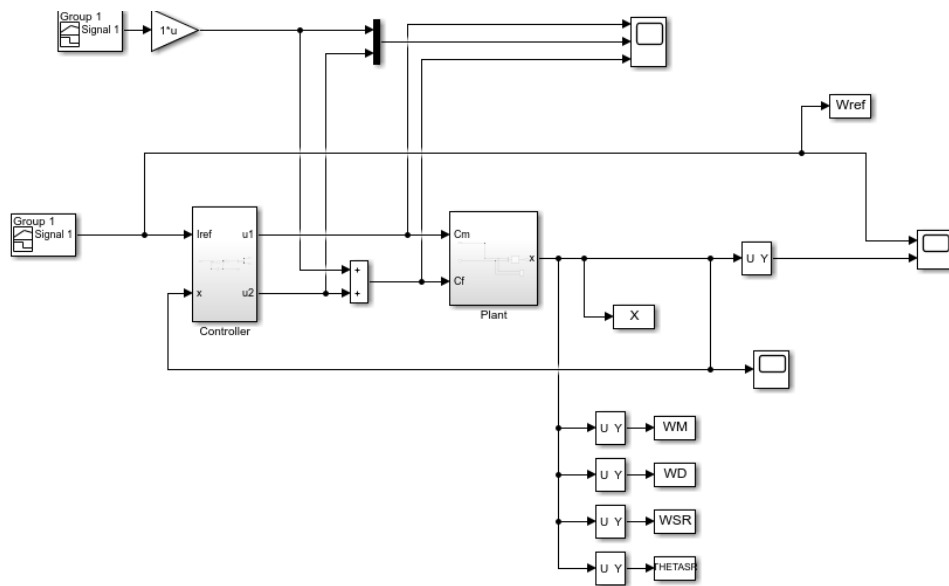
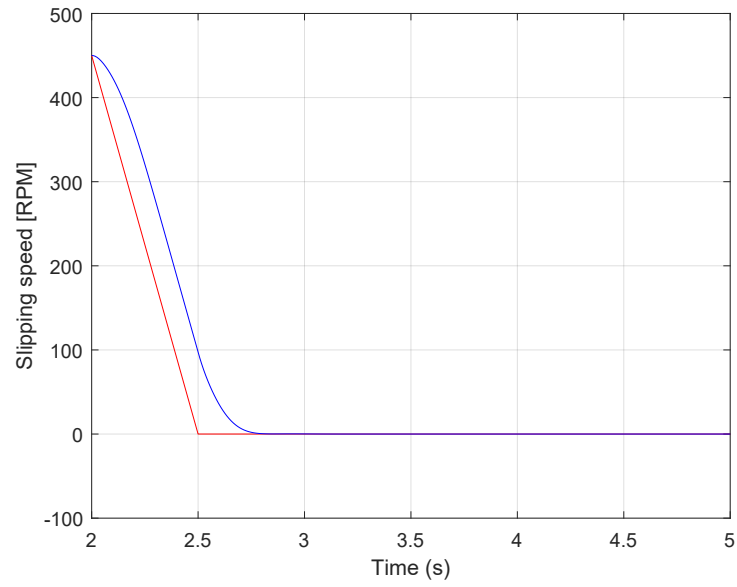
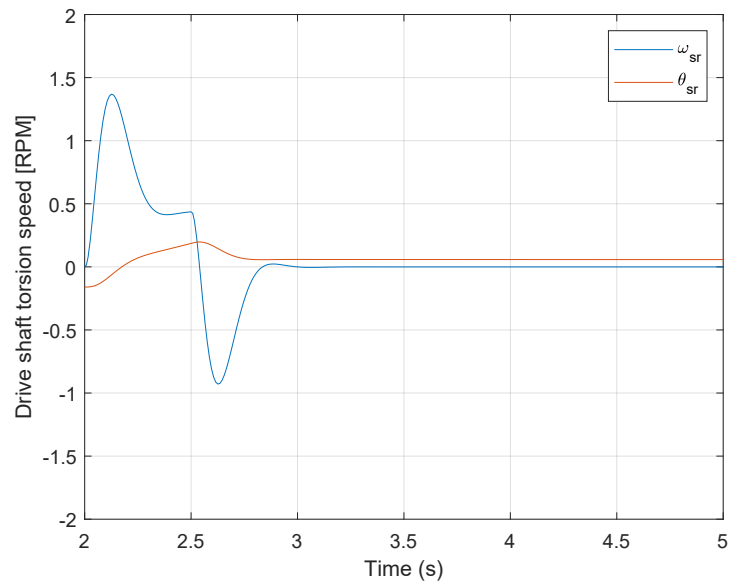


Figure 4.9: General scheme with controller



**Figure 4.10:** Delta speed behavior without actuators



**Figure 4.11:** Drive shaft torsion speed and angle

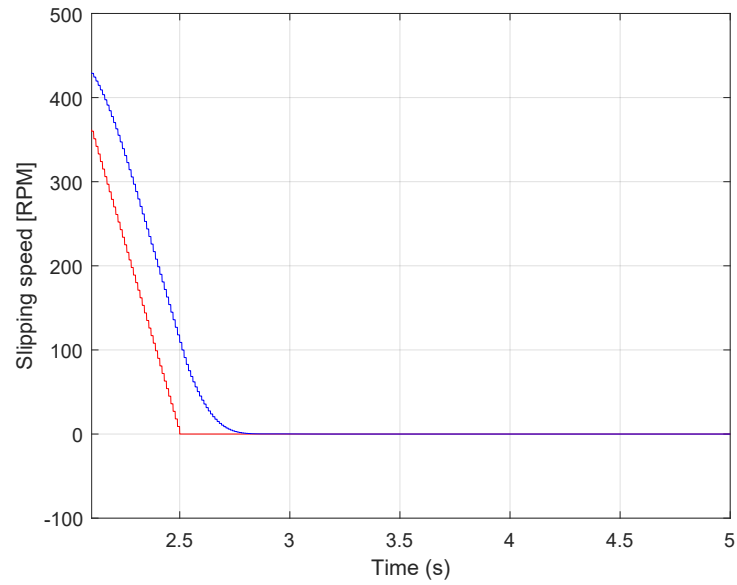


Figure 4.12: Delta speed behavior without actuators  $T=10\text{ms}$

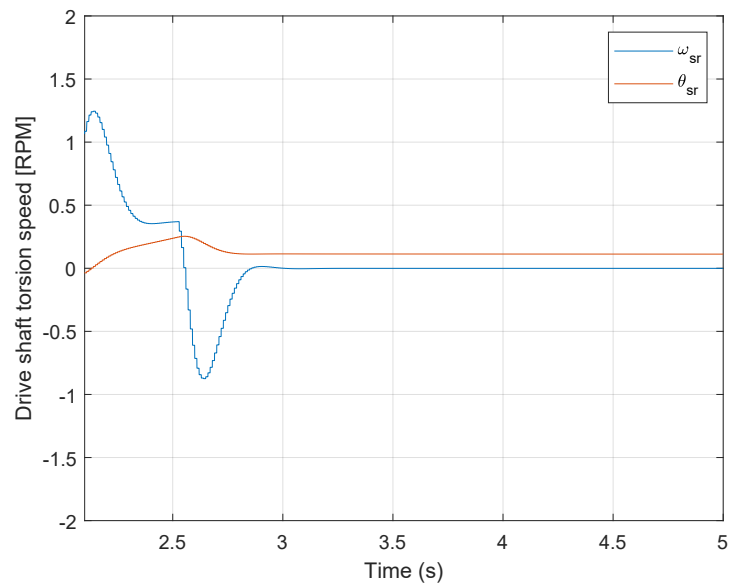
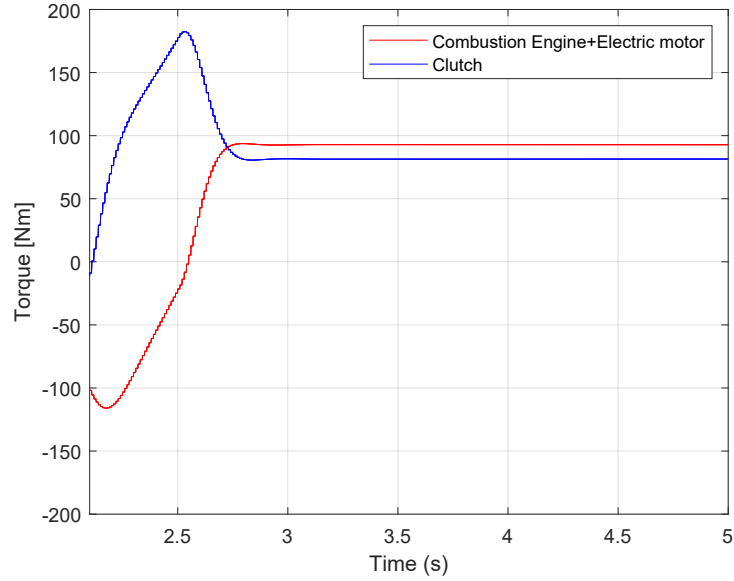


Figure 4.13: Drive shaft torsion speed and angle  $T=10\text{ ms}$



**Figure 4.14:** Total engine and clutch torque  $T=10$  ms

The controller performance is very good, the control targets are reached, but the model is different from the reality because all the effects of the actuators and their delays are here neglected.

In the following section more realistic models will be described together with the control strategies adopted in order to compensate the delays.

In order to evaluate the goodness of a method, the convergence speed of the primary output is not the only parameter to take into account: the amplitude of the oscillations is an important parameter too. In particular, the time interval between the starting control time ( $t_s = 2$ s) and the time  $t_f$  when the slipping speed  $\omega_d$  reaches the null value, is considered. With respect to the oscillations, the standard deviation  $\sigma$  is considered [11]: it is a measure of the variation/dispersion of a set of data with respect to the mean value. A low standard deviation indicates that the data points tend to be close to the mean of the set, while a high standard deviation indicates that the data points are spread out over a wider range of values. The standard deviation formula is the following:

$$\sigma = \frac{\sqrt{\sum_{i=1}^N (x_i - \mu)^2}}{N} \quad (4.36)$$

Another index used in order to evaluate the performance of a certain control strategy is the Root Mean Square Error.

The root-mean-square deviation (RMSD) [12] or root-mean-square error (RMSE) is a frequently used index used to measure the differences between values that can be population values or samples, predicted by a model and the values observed. The root mean square error represents "the square root of the second sample moment of the differences between predicted values and observed values or the quadratic mean of these differences". These quantities are called errors (or prediction errors) when computed out-of-sample and are considered residuals when the calculations are performed over the data sample that was used for estimation. The RMSE is used to evaluate the magnitudes of the errors in predictions for various times into a single measure of predictive power. This is a measure of accuracy and scale-dependent used to compare errors of different models for a particular dataset and not between datasets. This index is always non-negative, and a null value would indicate a perfect fit to the data. Usually, a lower value is better than a higher one. It is not valid to do comparisons across different types of data because the measure is dependent on the scale of the numbers used. RMS deviation is "the square root of the average of squared errors". The consequence of each error on RMSD depends on the size of the squared error so that larger errors have a very large effect on RMSD. It is important to remind that the Root Mean Square error is sensitive to outliers.

## Chapter 5

# Tuning and Simulation results

### 5.1 LQI technique with actuators and delays

In order to analyse a more realistic model, the engine and clutch actuators are introduced in before the plant with their respective delays. In this case the actuators transfer functions are not included in the plant model but the model itself is fed with the two inputs  $C_m$  and  $C_f$  after the actuation:

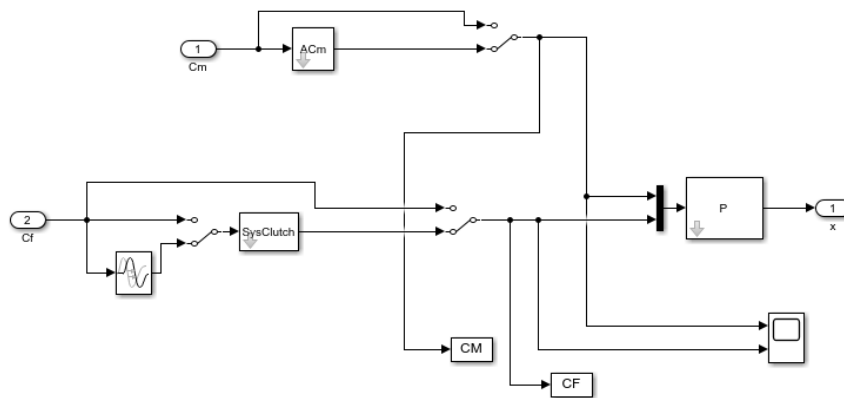


**Figure 5.1:** Plant fed with the actuated inputs

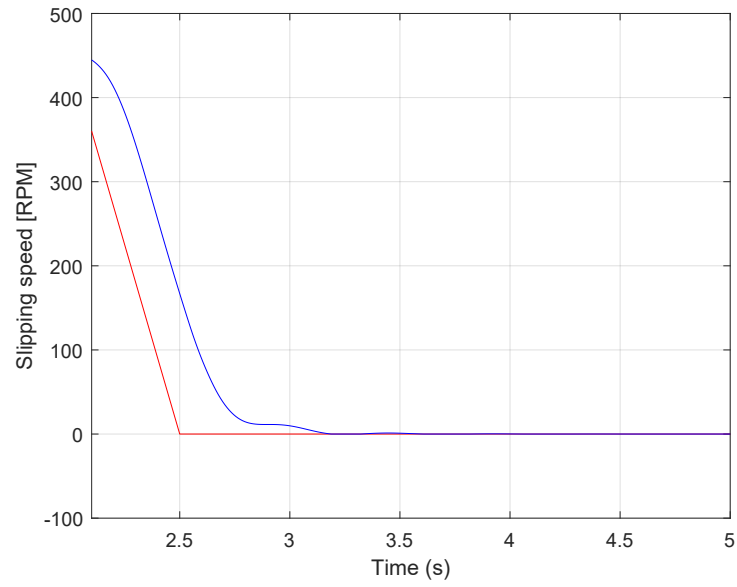


**Figure 5.2:** Delta speed behavior

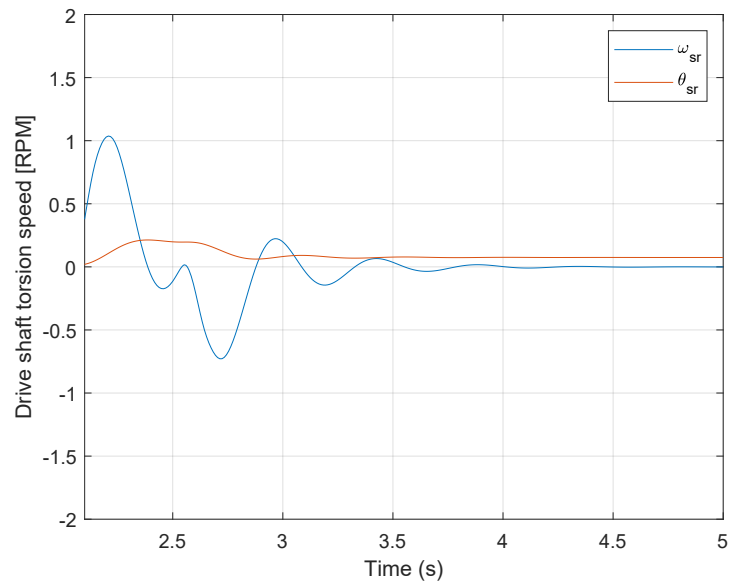


**Figure 5.3:** Drive shaft torsion speed and angle

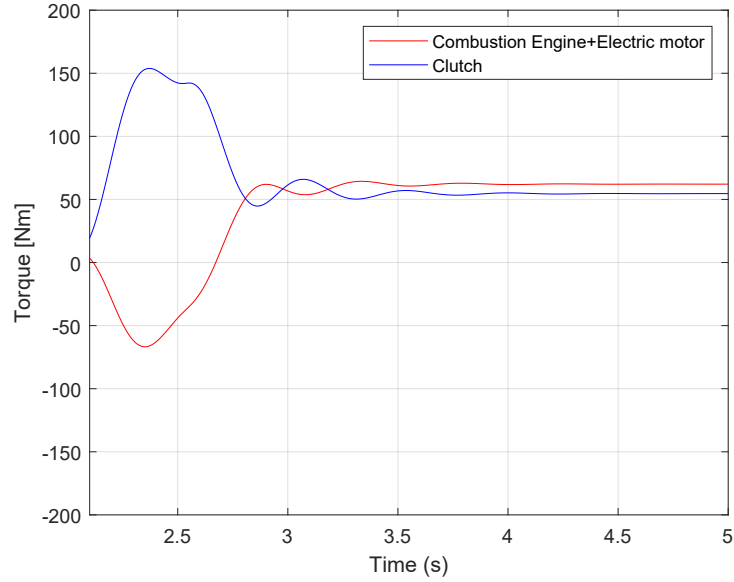


**Figure 5.4:** Total engine and clutch torque

As it is possible to observe in the figures above, the performance of the controller is deteriorated because of the introduction of the actuators with the respective delays. A new tuning of the weight matrices  $Q$  and  $R$  is here necessary.

Many processes involve dead times, also referred to as transport delays or time lags. Controlling such processes is challenging because delays cause linear phase shifts that limit the control bandwidth and affect closed-loop stability.

The  $Q$  and  $R$  weight matrices used to obtain the result are the following ones:

$$Q = \begin{bmatrix} 0 & 0 & 0 & 0 & 0 \\ 0 & 0.5 & 0 & 0 & 0 \\ 0 & 0 & 0 & 0 & 0 \\ 0 & 0 & 0 & 0 & 0 \\ 0 & 0 & 0 & 0 & 30 \end{bmatrix}$$

$$R = \begin{bmatrix} 0.2 & 0 \\ 0 & 0.2 \end{bmatrix}$$

The results are also derived in discrete time with  $T=10$  ms.

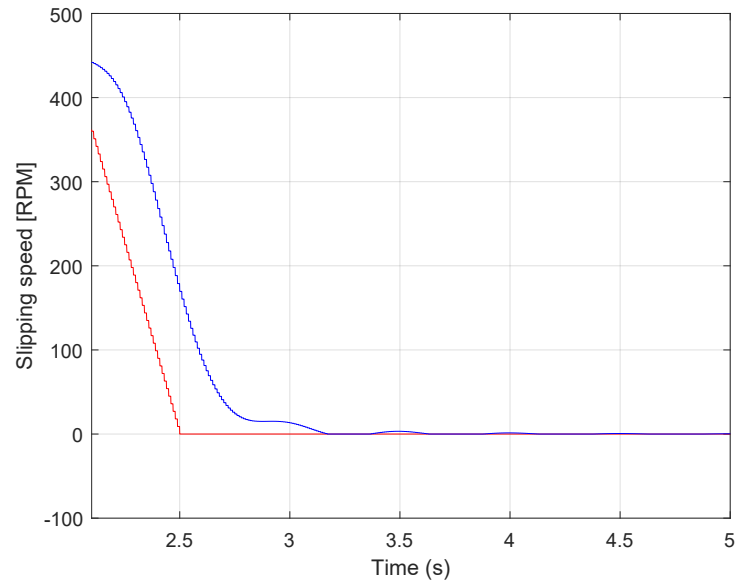


**Figure 5.5:** Delta speed behavior with  $T=10$  ms

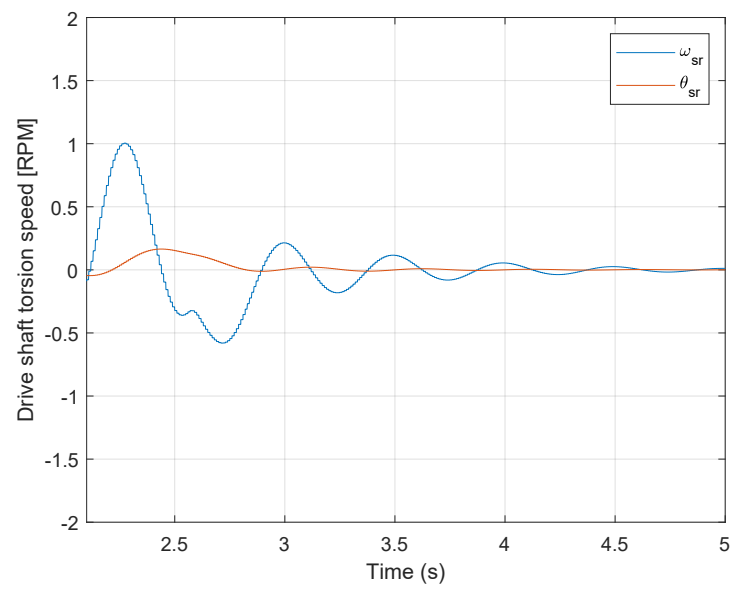


**Figure 5.6:** Drive shaft torsion speed and angle with  $T=10$  ms

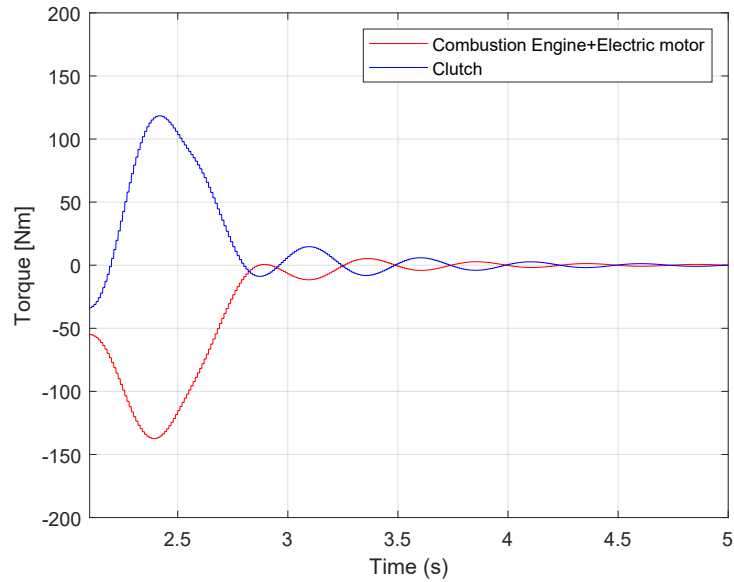


**Figure 5.7:** Total engine and clutch torque with  $T=10$  ms

As it is possible to observe from the graphs above, the discretization of the control at  $T=10$  ms, deteriorates the performance, also because of the introduction of the actuators and the delays in the model.

In order to solve the problem, other techniques are introduced together with the Linear Quadratic Integral control, the actuators are involved into the plant model and predictors for their states are then introduced to observe them.

## 5.2 Linearization of the actuators and delays

The effects of the delays of the engine and clutch actuators in the control are minimized linearizing the entire model plant:

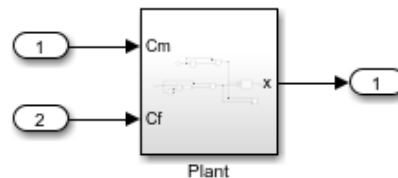


**Figure 5.8:** Model plant to be linearized

The linearization is computed through the Matlab command *linmod* that computes a linear state-space model by linearizing each block in a model individually. This command obtains linear models from systems of ordinary differential equations described as Simulink models. Inputs and outputs are denoted in Simulink block diagrams using Inport and Outport blocks.

The default algorithm uses preprogrammed analytic block Jacobians for most blocks which should result in more accurate linearization than numerical perturbation of block inputs and states.

The purpose of the *linmod* function is to obtain a linearized model of a nonlinear system. Linear approximations are much more desirable to work with since it is possible to predict the behavior of linear systems. Nonlinear systems exhibit behavior which can be radically different for different inputs, making them difficult to control. This is accomplished by approximating the behavior of a nonlinear system in a limited range of operation. This range of operation may be considered the operating point of the system being linearized. Dealing with nonlinearity in a system is not an easy task. The difficulty in linearizing a nonlinear system increases with the amount of nonlinearity. In other words, systems described by higher order polynomials are more difficult to linearize than systems which can be represented by lower order polynomials.

The limit of this kind of control is that the state space representation derived contains also the states of the actuators that are not measured: in order to solve this problem other techniques are introduced to observe them.

The performance in terms of delta speed behavior, drive shaft torsion speed and engine and clutch torque is shown below:

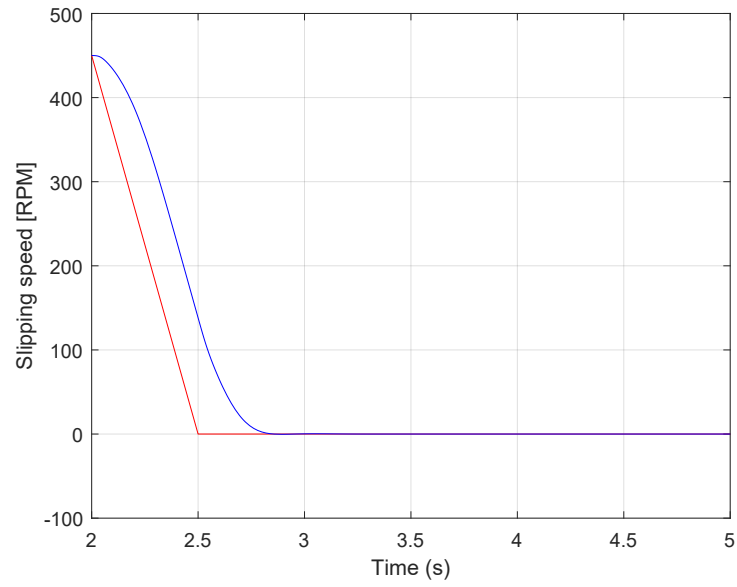


**Figure 5.9:** Delta speed behavior with linearization

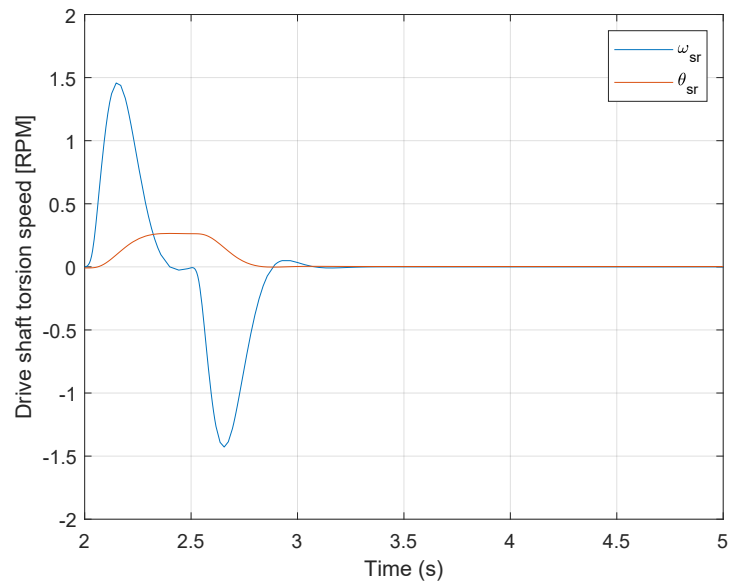


**Figure 5.10:** Drive shaft torsion speed and angle with linearization

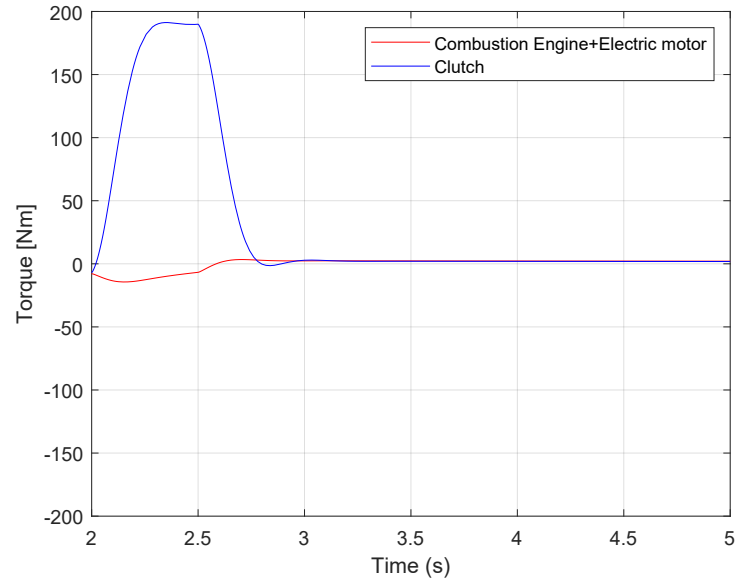


**Figure 5.11:** Total engine and clutch torque with linearization

As it is possible to observe from the figures above, the approach of delta speed to zero is not abrupt and undesired oscillations are avoided.

After  $\omega_d$  reaches the zero value, there are not oscillations of the torsion speed and angle.

The control is also performed discretizing at  $T=10$  ms.

The discretization seems not to cause any loss of performance of the control, even if an accurate comparison will be shown later, calculating the values of the standard deviation and Root Mean Square Error together with the convergence time  $\Delta t$ .

The performance of this technique is very good except for the fact that the control of the states of the actuators that cannot be measured is here done through a trial and error procedure.

After the linearization, an attempt for reducing the computational complexity of the model is performed, obtaining results full of oscillations for the torsion speed and a long time of convergence for  $\omega_d$ , so the technique is not taken into account in this dissertation.

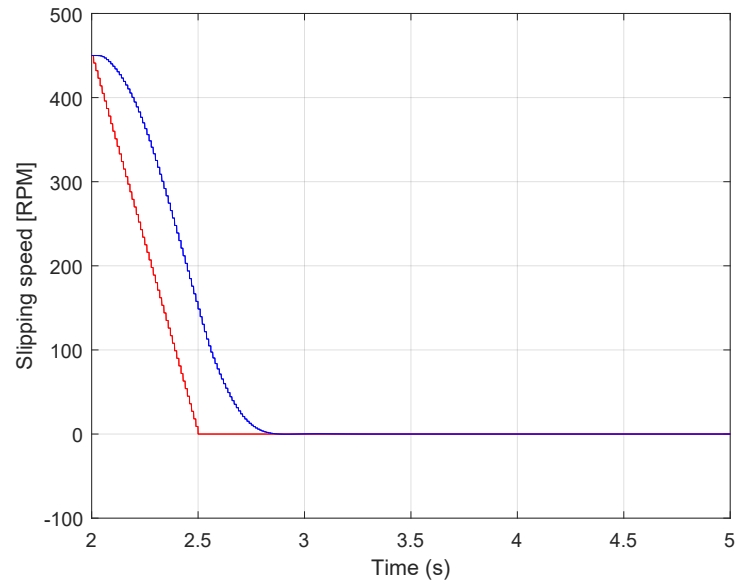


**Figure 5.12:** Delta speed behavior with linearization  $T=10$  ms

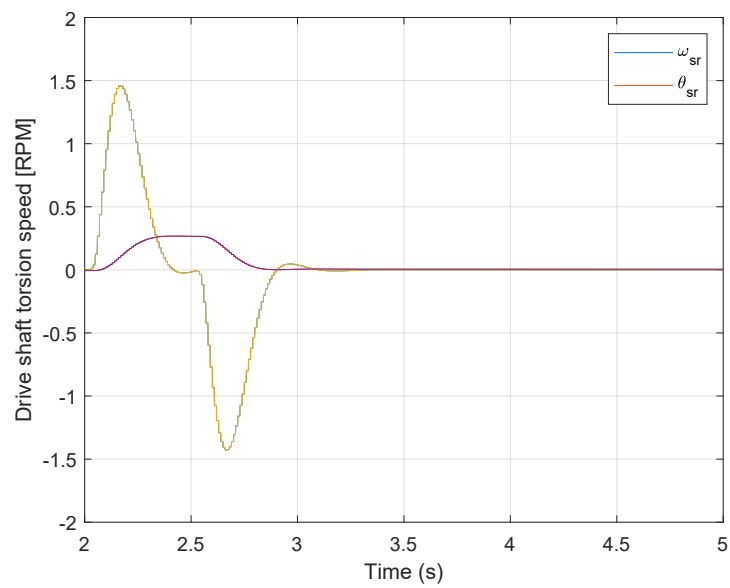


**Figure 5.13:** Drive shaft torsion speed and angle with linearization  $T=10$  ms

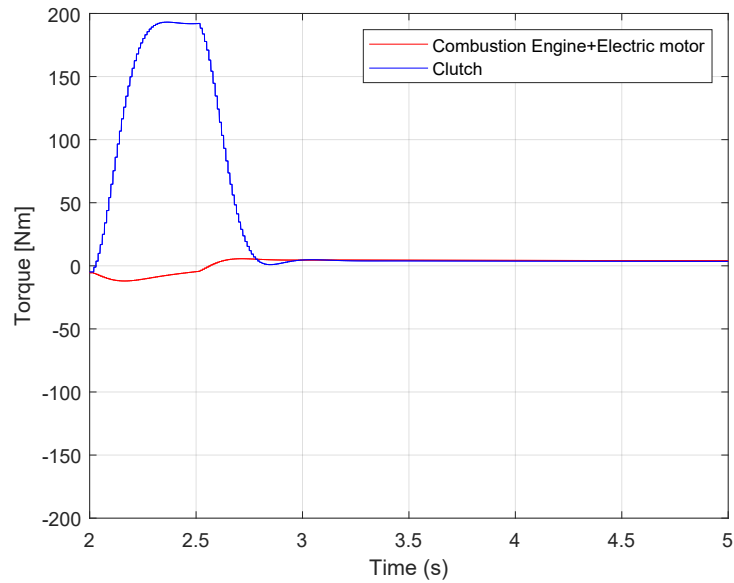


Figure 5.14: Total engine and clutch torque with linearization  $T=10$  ms

### 5.3 LQI technique with Smith Predictor

In order to manage the delay of the clutch actuator, that causes some problems in the tuning of the  $Q$  and  $R$  matrices, its transfer function is considered as a secondary plant to be controlled using the Smith Predictor. The Simulink Scheme is shown below:

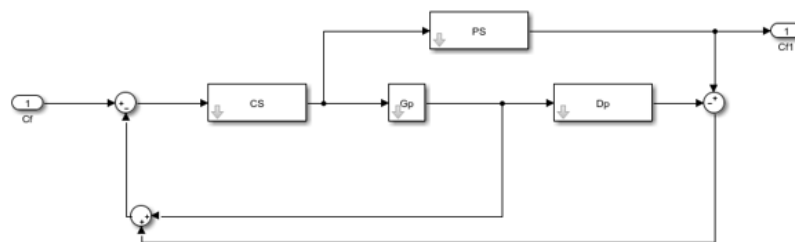
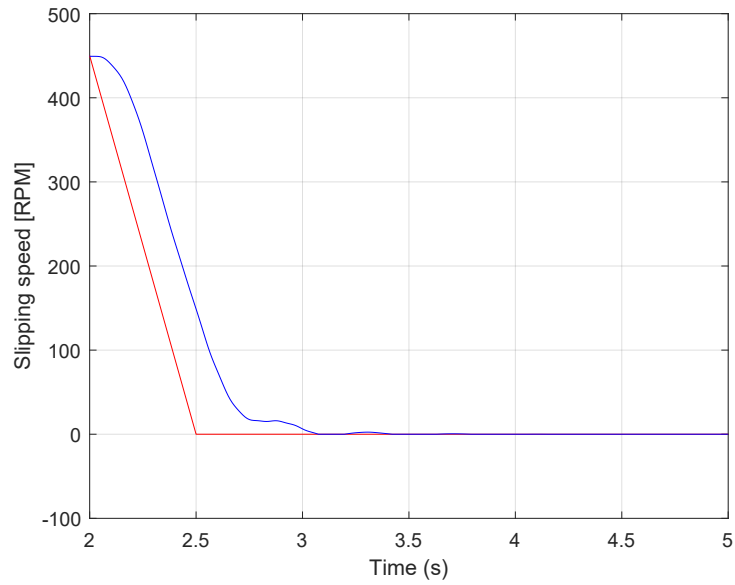
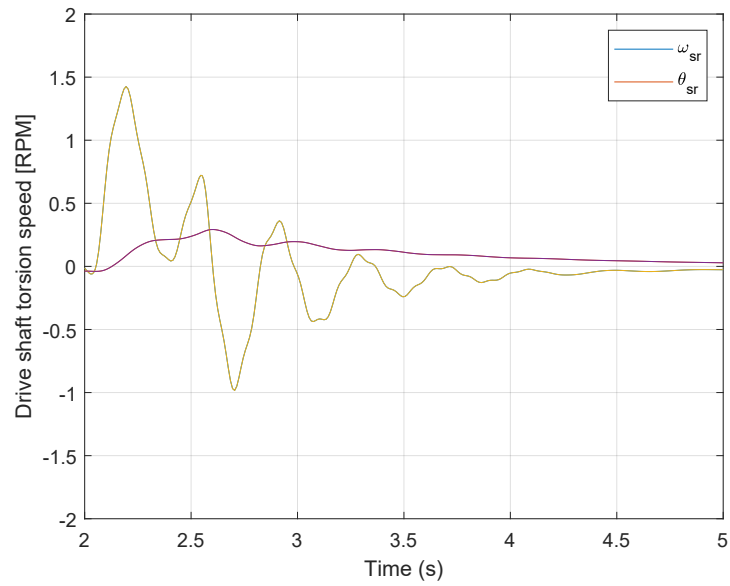


Figure 5.15: Smith Predictor scheme for clutch actuator

Where  $CS$  is the controller,  $Gp$  is the actuator transfer function without the delay,  $PS$  is the plant of the actuator with delay and  $Dp$  is the delay itself. The controller adopted here is a PI controller.



**Figure 5.16:** Delta speed behavior with LQI and Smith Predictor



**Figure 5.17:** Drive shaft torsion speed and angle with LQI and Smith Predictor

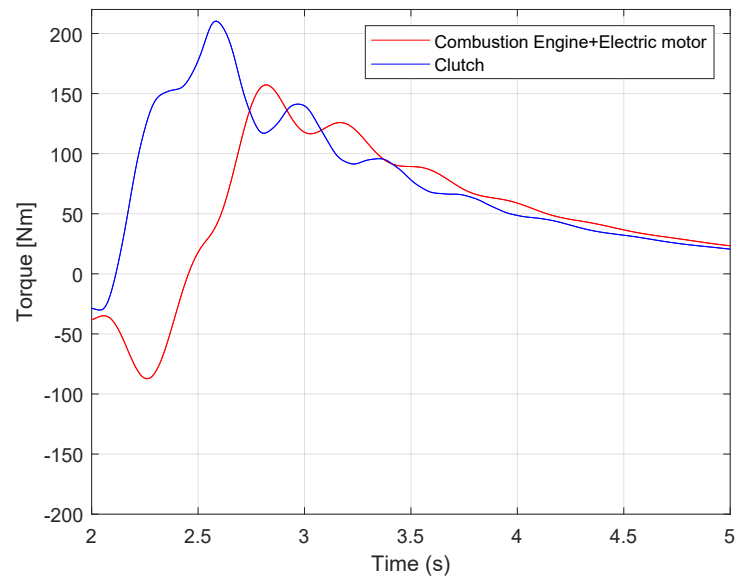


**Figure 5.18:** Total engine and clutch torque with LQI and Smith Predictor

As it is possible to observe the results are good in terms of delta speed convergence, even if there are some oscillations in the torsion speed. The correct estimation of the performance will be done later through the computation of the RMSE and standard deviation but in general, the results obtained seem to be worse than those obtained before, through the linearization of the entire model.

Even when  $\omega_d$  reaches the null value, some oscillations are present and this behavior represents a loss of performance of the LQI controller.

## 5.4 State space representation of the actuators and the Plant with LQI technique

As explained in chapter 3, section 3.3, the final shape of the state space representation is here derived, where the outputs of the actuators become the inputs of a new augmented plant with 9 states described by the matrices  $\bar{A}$  and  $\bar{B}$ .

$$\bar{A} = 10^4 \begin{bmatrix} 0 & 0 & 0 & 0 & -0.0013 & 0.0001 & -0.0004 & -0.0026 & 0.0014 \\ 0.0001 & -0.0001 & 0.1117 & 7.1500 & -0.0327 & 0.0030 & -0.0091 & -0.0675 & 0.0014 \\ 0 & 0 & -0.012 & -0.7696 & 0.0034 & -0.0003 & 0.0009 & 0.0069 & 0 \\ 0 & 0 & 0.0001 & 0 & 0 & 0 & 0 & 0 & 0 \\ 0 & 0 & 0 & 0 & -0.0216 & -0.022 & -0.0118 & -0.0052 & 0 \\ 0 & 0 & 0 & 0 & 0.0256 & 0 & 0 & 0 & 0 \\ 0 & 0 & 0 & 0 & 0 & 0.0128 & 0 & 0 & 0 \\ 0 & 0 & 0 & 0 & 0 & 0 & 0.0064 & 0 & 0 \\ 0 & 0 & 0 & 0 & 0 & 0 & 0 & 0 & -0.0014 \end{bmatrix} \quad (5.1)$$

$$\bar{B} = \begin{bmatrix} 0 & 0 \\ 0 & 0 \\ 0 & 0 \\ 0 & 0 \\ 8 & 0 \\ 0 & 0 \\ 0 & 0 \\ 0 & 0 \\ 0 & 4 \end{bmatrix} \quad (5.2)$$

The Simulink scheme of the complete model is shown below:

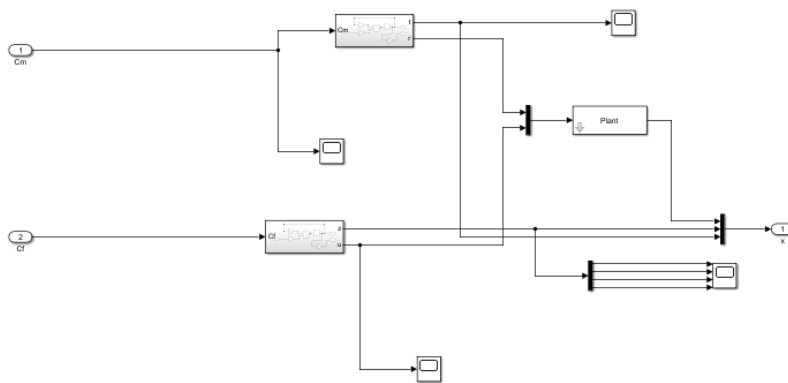


**Figure 5.19:** Simulink scheme of the complete system

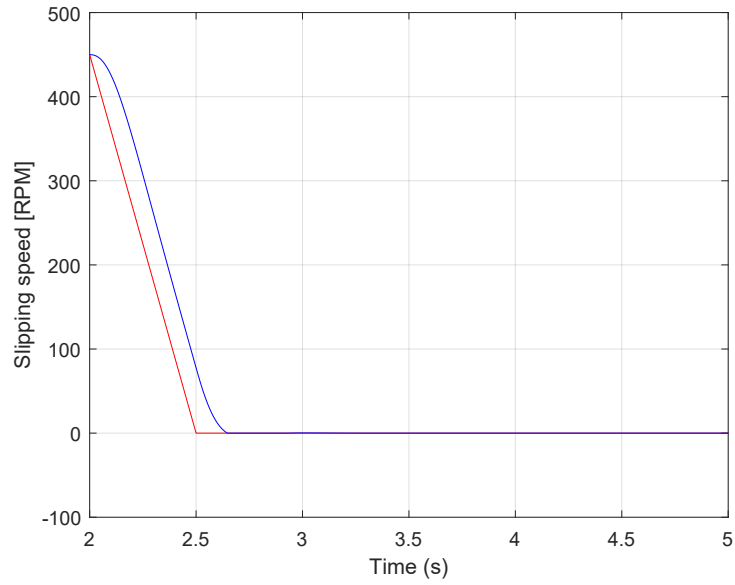


**Figure 5.20:** Delta speed behavior with LQI and complete State Space

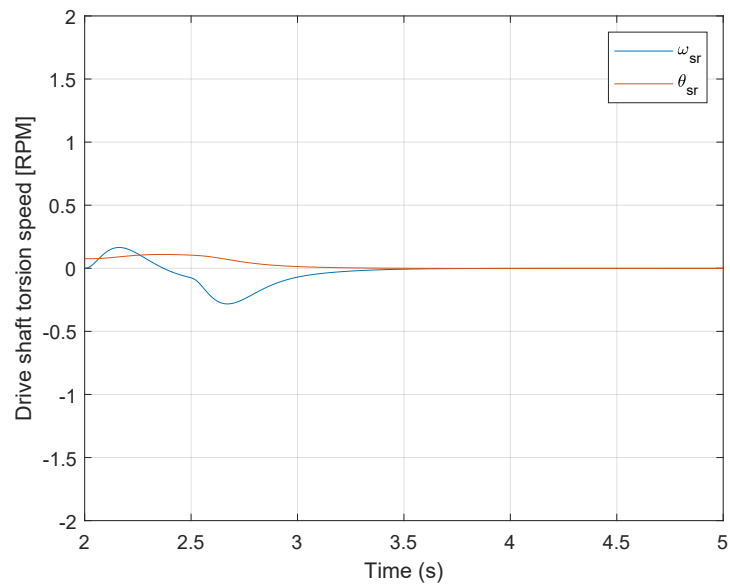


**Figure 5.21:** Drive shaft torsion speed and angle with complete State Space

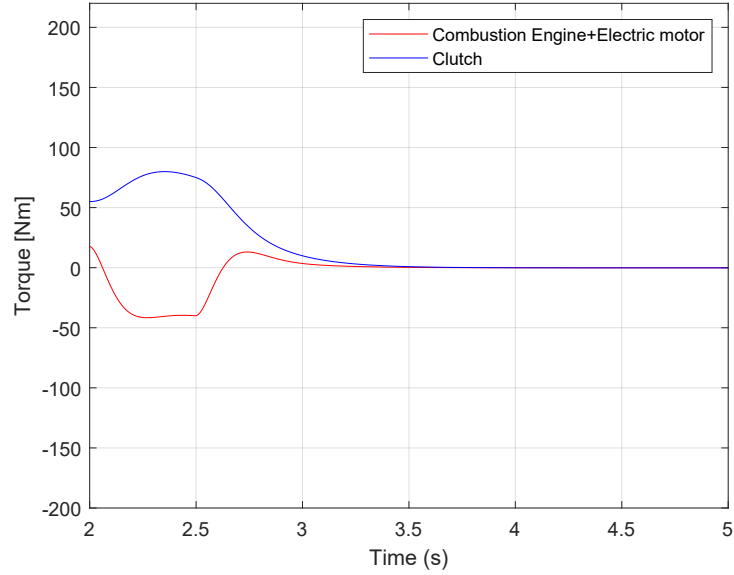


**Figure 5.22:** Total engine and clutch torque with LQI and complete State Space

The computation of a state space representation of the model including the transfer functions of the actuators and delays makes possible the development of a more robust and accurate control of the system that takes into account all the uncertainties. As it is possible to observe from the figures shown above, the performance is very good, the oscillations of the drive shaft torsion speed and angle are reduced to the minimum and the delays of the actuators are managed avoiding problems in the control.

The final way in order to manage the states of the actuators that cannot be measured is that to associate to this kind of control with this state space representation the Kalman Filter for the three subsystem of the model that are the plant itself and the two actuators.

This will be the last step in the research of an optimal usage of the LQI control strategy for the Dry Dual Clutch Transmission avoiding oscillations and a smooth convergence of the value of  $\omega_d$  that is the most important control target.

## 5.5 Kalman State Estimation

The observation of the states of the actuators is then implemented in Simulink realizing a Kalman filter design for each single plant of the complete system.

The Kalman filter is designed for the clutch and engine actuators: the plant contains their outputs as inputs.

In this way the performance of the control is improved and also the tuning of the Q and R matrices becomes simpler. The weights for the actuators states are tuned inside the Q and R matrices of the Kalman Filter.

The Simulink scheme is shown below:

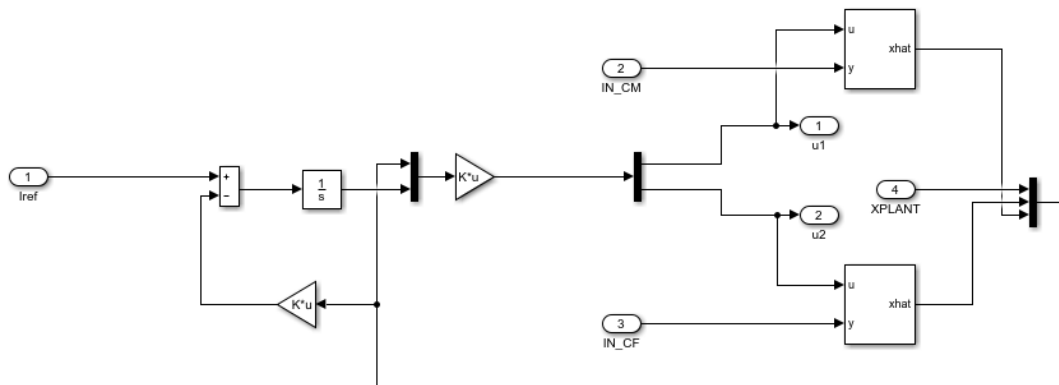


Figure 5.23: LQI with Kalman filter

The results of this kind of control are very good in terms of convergence of  $\omega_d$  even if the interval is longer than the previous model but also in terms of the oscillations given by the torsion angle that here remains close to the null value.

It is possible to observe that the controller, computing properly the clutch and the engine torque, is able to ensure a smooth tracking of the reference clutch slipping speed in order to improve driver comfort and drivability.

The expected performance is reached in the best way adopting the LQI control strategy together with the Kalman filter.

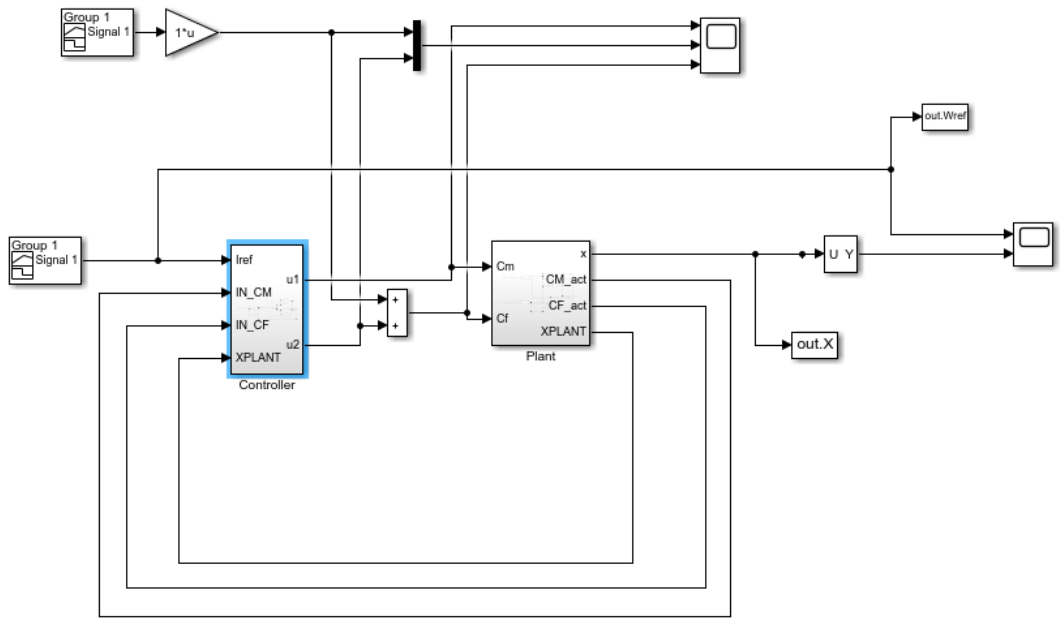


Figure 5.24: Full model with observer

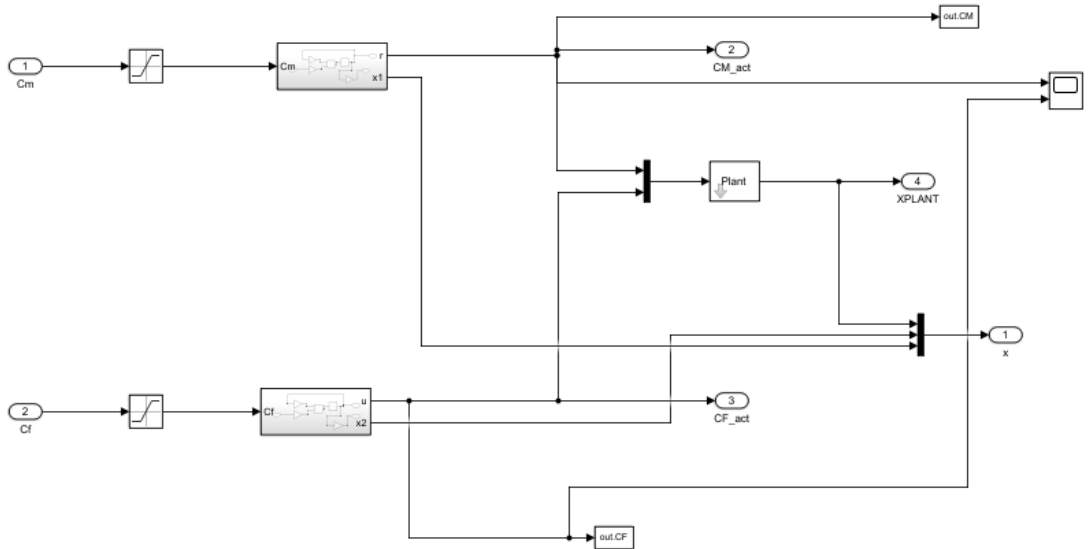
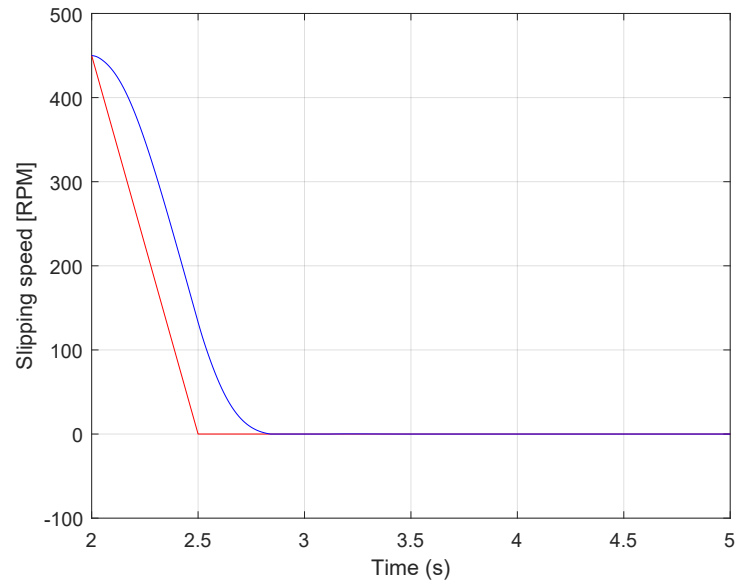
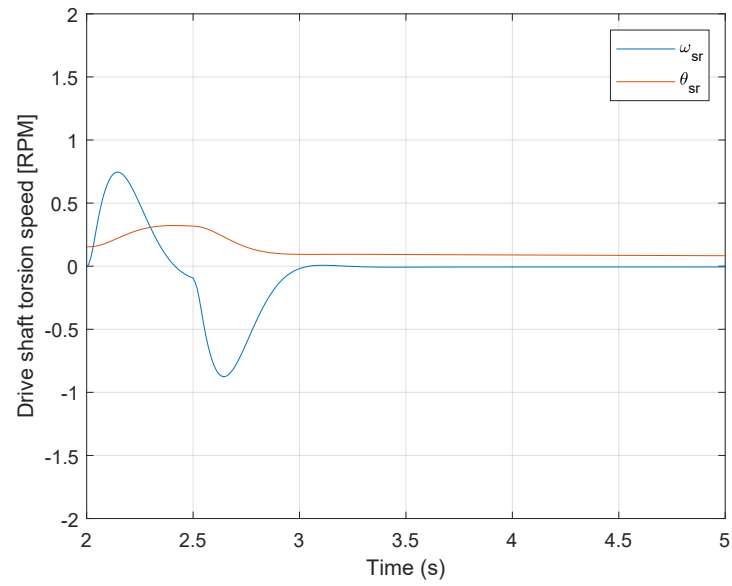


Figure 5.25: Plant with actuators



**Figure 5.26:** Delta speed behavior with LQI and Kalman filter



**Figure 5.27:** Drive shaft torsion speed and angle and Kalman filter

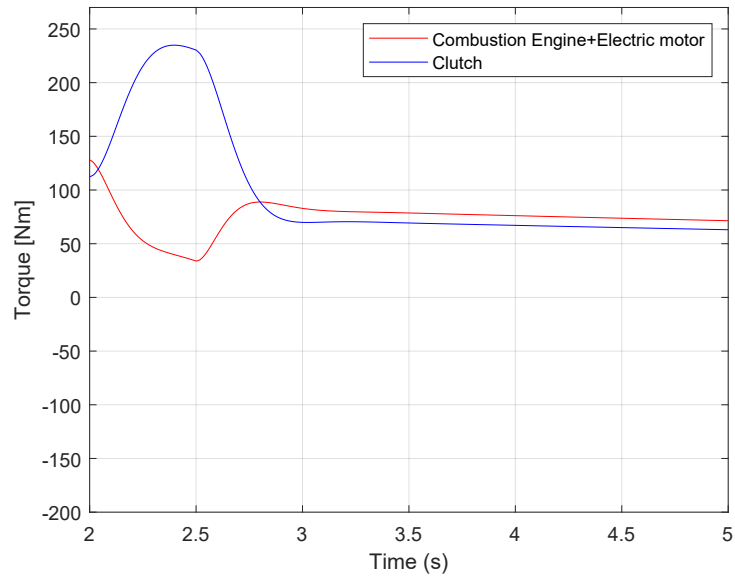


Figure 5.28: Total engine and clutch torque with LQI with Kalman filter

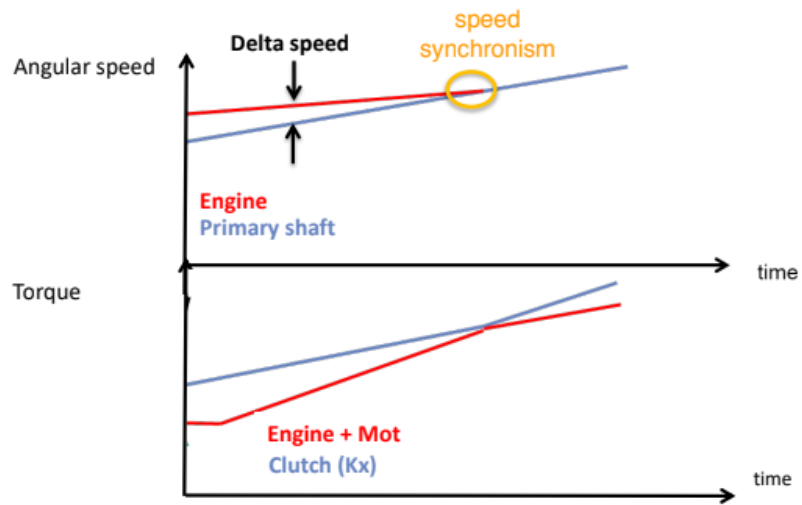


Figure 5.29: Expected performance

## 5.6 Comparison between simulation results

In this section comparisons between the obtained results are shown, with the aim of understanding which is the model and the control strategy that ensures best performances.

With respect to the oscillations, the standard deviation  $\sigma$  is considered: it is a measure of the variation/dispersion of a set of data with respect to the mean value. In particular, the time interval between the starting control time ( $t_s = 2s$ ) and the time  $t_f$  when the slipping speed  $\omega_d$  reaches the null value, is considered.

With respect to the oscillations, the standard deviation is considered: it is a measure of the variation/dispersion of a set of data with respect to the mean value.

The slipping speed analysis is done in terms of RMSE and standard deviation in order to have a correct evaluation of the dispersion of the data.

The values are computed through the commands "*rms*" and "*std*" given by Matlab and all the quantities are considered after the starting of the control so at  $t_s=2s$ .

Model	$\sigma_{\omega_{sr}}$	$\sigma_{\omega_d}$	RMSE $\omega_d$
LQI without actuators	0.36	125.05	137.03
LQI with actuators and delays	0.28	144.00	163.30
LQI with linearization	0.58	180.35	247.40
LQI with Smith Predictor	1.81	140.35	158.17
LQI State Space Representation of the plant and actuators	0.08	121.43	134.20
LQI with Kalman Filter	0.28	122.4	135.00

**Table 5.1:** Indices computation

Model	$\Delta t$
LQI without actuators	0.72
LQI with actuators and delays	1.59
LQI with linearization	0.90
LQI with Smith Predictor	1.38
LQI State Space Representation of the plant and actuators	0.70
LQI with Kalman Filter	0.85

**Table 5.2:** Convergence interval

### **5.6.1 Observations**

The convergence time is a very important parameter in the evaluation of the performance of a certain control strategy. If  $\omega_d$  reaches the null value before, a faster tracking of the slipping speed reference signal is guaranteed.

As it is possible to observe, the LQI full model with actuators and delays has the lowest convergence interval and also the other indices demonstrate that it represents the best control strategy developed in this thesis even if it is not so realistic because this model does not consider the fact that the states of the actuators cannot be measured.

The adoption of the Smith Predictor significantly reduces the convergence interval but causes a lot of oscillations as it is possible to see in the high values of the standard deviation of  $\omega_{sr}$  and also from the indices calculated for the slipping speed.

The state space representation of the entire model with the actuators increases a lot the performances also with a trial and error regulation of the weight matrices for the states of the actuators. The full model without observers guarantees a good trade off between time convergence and oscillations even if it is not possible to measure the states of the actuators included in the control. This leads to the adoption of the Kalman Filter to correctly estimate them.

In this way, the performance deteriorates a little bit, but the model is coherent with the unmeasurability of the states of the actuators.

# Chapter 6

## Conclusions

This thesis has dealt with the control of the dry dual clutch during its slipping phase. In particular, the main purpose of the project has been to design a controller that, computing properly the clutch and the engine torque, is able to ensure a smooth tracking of the reference clutch slipping speed in order to improve driver comfort and drivability.

The Linear Quadratic Integral control technique has been used: it has been described from a theoretical point of view, then the advantages of using this technique have been explained; in particular the main reason is represented by the fact that this method is more flexible with respect to more traditional techniques.

In this regard, different configurations have been used in order to exploit the possible advantages caused by different control strategies. As a starting point, a model without the clutch and engine actuators and delays has been considered. Then these parts have been introduced in order to represent the real model with its uncertainties : the tuning of the matrices has become more difficult and oscillations have been introduced in the behavior of the  $\omega_d$  and  $\omega_{sr}$ .

In addition to the basic model, the engine torque actuator and the clutch torque one have been inserted in Simulink and subsequently some ways to compensate them have been experimented.

For all the investigated configurations simulation results corresponding to different controller parameters settings have been presented. The best set of parameters used for simulations have been chosen after performing an extensive tuning procedure: the full LQI model with actuators and delays ensures the most satisfactory performances.

In particular, it is shown that the LQI with actuators and delays has the worst performance in terms of convergence interval even if the drive shaft torsion speed and angle are comparable with the control without actuators.

In changing the configurations of the model, the kind of control turns out to be very flexible since it can be used through a general approach also introducing other compensations for the delays.

In the end some important indices have been calculate in order to realize an analysis of the performance: the main purpose was to show that there is always a trade-off between the oscillations and the time convergence. By observing simulation results it is clear that the configuration with the state space representation of the plant and the two actuators with Kalman Filter ensures very good results in terms of slipping speed reference tracking and oscillations reduction considering also the fact that this is the most realistic configuration.

The discretization of the control to  $T=10$  ms strategy does not bring significant modifications in terms of performances: the most important elements in this regard are instead represented by a correct tuning of the weight matrices  $Q$  and  $R$ .

## 6.1 Future works

Starting from the results presented in this thesis project, further studies can be conducted and different applications can be explored.

In particular it is possible to:

- evaluate the performance in terms of vehicle acceleration and drivability;
- compute the feedforward contribution of the engine torque with the inversion on the model and using the the generated references as inputs of the inverse model;
- use the driver torque (that is function of the accelerator pedal) as feedforward contribution for the clutch torque command.

It is also possible to validate the control experimenting it on vehicle.

# Bibliography

- [1] F. Cimmino C. Vafidis. «FPT's High Torque Density Dual Clutch Transmission(HTDDCT)». In: 8th CTI Symposium Innovative Automotive Transmissions (Berlin,2009) (cit. on p. 1).
- [2] Ioan-Adrian Viorel Loránd Szabò Lars Lowenstein Cristian Stet. «Integrated starter-generators for automotive applications». In: Volume 45, Number 3 (2004) (cit. on p. 5).
- [3] A. Bordoni G. Gatti. «Development of Fiat powertrain new C725 7-Speed dual dry clutch transmission for FWD passenger vehicles». In: (Shangai,2013) (cit. on p. 12).
- [4] T. Jin P. Li G. Zhu. «Optimal decoupled control for dry clutch engagement». In: American Control Conference (ACC), pages 6740-6745 (2013) (cit. on p. 17).
- [5] P. J. Dolcini C. Canudas-de Wit H. Béchart. «Dry clutch control for automotive applications». In: Springer Science and Business Media (2010) (cit. on p. 18).
- [6] L. Glielmo L. Iannelli V. Vacca F. Vasca. «Gearshift control for automated manual transmissions». In: IEEE/ASME Transactions on, 11(1):17–26 (2006) (cit. on p. 18).
- [7] Jinsung Kim Kwanghyun Cho Seibum B. Choi. «Gear Shift Control of Dual Clutch Transmissions with a Torque Rate Limitation Trajectory». In: American Control Conference on O'Farrell Street, San Francisco, CA, USA (June 29 - July 01, 2011) (cit. on p. 19).
- [8] Massimo Canale. «Slides of the course». In: Digital control systems and architectures (2019) (cit. on p. 32).
- [9] Angelo Salatino. «Notes on Smith Predictor». In: Metodi di controllo per i sistemi di elaborazione e comunicazione (2012) (cit. on p. 38).
- [10] Carlo Novara. «Slides of the course». In: Nonlinear control and aerospace applications (2018-2019) (cit. on p. 41).

*BIBLIOGRAPHY*

---

- [11] Bland J.M. Altman D.G. «Statistics notes: measurement error». In: *BMJ* (1996) (cit. on p. 47).
- [12] Hyndman Rob J. Koehler Anne B. «Another look at measures of forecast accuracy». In: *International Journal of Forecasting* (2006) (cit. on p. 48).